The North African Journal of Scientific Publishing (NAJSP)
مجلة شمال إفريقيا للنشر العلمي (NAJSP)
E-ISSN: 2959-4820
Volume 3, Issue 3, 2025
Page No: 169-198
Website: https://najsp.com/index.php/home/index
SJIFactor 2024: 5.49 معامل التأثير العربي (AIF) 2024: 0.71 ISI 2024: 0.696

A Review of Current Mode Filter Design using Current Conveyor and its Variants

Musa Ali Albrni[1*], Mansur Ali Jaba[2], Aadel Fathe Howedi[3], Majdi Ibrahim Alashhb[4]
[1,2,3]Higher Institute of Engineering Technology, Zliten, Libya
[4]Faculty of Information Technology, Alasmarya Islamic University, Zliten, Libya

مراجعة تصميم المرشحات باستخدام ناقل التيار (CC) ومتغيراته:

موسى علي البرني[1*]، منصور علي جابة[2]، عادل فتحي هويدي[3] مجدي ابراهيم الأشهب[4]
[1,2,3]المعهد العالي للتقنيات الهندسية، زليتن، ليبيا
[4]كلية تقنية المعلومات، الجامعة الأسمرية الإسلامية، زليتن، ليبيا

*Corresponding author: Mansurjaba@gmail.com

Received: July 01, 2025	Accepted: August 06, 2025	Published: August 16, 2025

Abstract:
Several current-mode all inclusive channels that are based on diverse sorts of current transports are investigated. The filters are divided into two groups: single input multi output (SIMO) filters and multi input single output (MISO) and multi input multi output (MIMO) filters. Filter categorization and design restrictions are discussed. Some current mode active elements with CCII in their main function are reportedly appropriate for filter implementation are briefly introduced. Based on answers obtained, the amount of grounded and floating elements employed, the ability to independently alter filter parameters, and programmability, twenty-five remarkable filter topologies are examined and contrasted. Additionally, covered is the significance of tuning capacity in filter topologies.

Keywords: Current Mode; Universal Filter; Current Conveyor; Digitally Programmable.

الملخص
تم استعراض العديد من المرشحات العالمية بناءً على أنواع مختلفة من ناقلات التيار. قسمت المرشحات إلى مجموعتين: مرشحات المجموعة الأولى من نوع متعددة المدخلات وأحادية المخرج وأيضا متعددة المداخل والمخارج والمجموعة الثانية هي من نوع أحادية المدخل ومتعددة المخارج. ناقشت الدراسة أيضاً قيود التصميم وتصنيف المرشحات. كما قُدّمت مقدمة مقتضبة لبعض العناصر النشطة والتي تتكون بالأساس من نواقل التيار من الجيل الثاني والتي صُنّفت مناسبة لتطبيق المرشحات. تم دراسة خمسة وعشرون تصميماً للمرشحات، وقُورنت بناءً على الاستجابات المُحققة، وعدد العناصر المؤرضة والعائمة المُستخدمة، وإمكانية التحكم المُستقل في مُعاملات المرشح، وقابلية البرمجة. كما ناقشت الدراسة أهمية إمكانية الضبط في المرشحات.

الكلمات المفتاحية: نوع التيار؛ مرشح عالمي؛ ناقل التيار؛ قابل للبرمجة رقميًا

Introduction

Since analog filters are a crucial component of practically all electronic systems, the field of their s ynthesis and development is constantly changing. Among various filter structures universal filters (UFs) are the most versatile as all the standard filter functions can be derived from them [1-3]. They provide a stand-alone solution for a variety of filtering requirements. The UFs find applications in phase locked loop FM stereo demodulator, telephone decoder, speech processing etc, [4,5]. Low voltage operation capability with a suitable frequency response is now a must due to the widespread use of wearable biomedical devices and portable electronics [6–8]. Capacitor and/or resistor arrays were used in the

past to create filters, but their high-power consumption and requirement for a wide silicon area rendered them inappropriate for use in integrated circuit (IC) implementations today.

In terms of region effectiveness, moo voltage, moo control operation, and pertinence, dynamic element-based filters are the most engaging. Various filter topologies were developed utilizing operational intensifiers (OPAMPs), which revolutionized the field of filter planning. Current high-speed systems cannot use OPAMPs because of the narrow frequency range caused by the gain bandwidth constraint [3]. Additionally, compared to their current-mode counterparts, voltage-mode devices are thought to be less appealing for low voltage operation [3, 9, 10]. The latter have improved slew rate, a broad bandwidth, low chip area consumption, a simple architecture, good accuracy, and are less affected by supply voltage scaling [6]. Current mode devices are the perfect option for contemporary analog signal processing applications because of these characteristics.

The current conveyor and its variations are the most adaptable active element for the implementation of current mode filters [11–13]. Due to ongoing research in this area, many new current-mode elements have been proposed for filter realizations in recent years. Among the most commonly used active components are the first-generation current transport (CCI) [13] and the second-generation current transport (CCII) [13], current transport of the third era (CCIII) [14], current-controlled transport (CCCII) [15], current-controlled current transport transconductance speaker (CCCCTA) [16], completely differential current transport (FDCCII) [17], dual-X current transport (DX-CCII) [18], differential voltage current transport (DVCCII) [19], electronically flexible current transport (ECCII) [20], carefully programmable current transport (DPCC) [21], and so on. Filters created utilizing these dynamic components can be effectively found in existing writing [3,5,14-16,22].

This review article primarily concentrates on the examination of a select few notable current mode universal filter architectures. The filters examined in this study are categorized into two groups based on the number of input and output terminals: MIMO and SIMO. The article explores filter designs utilizing various current mode active components, with CCII serving as their foundation. Firstly, the design limitations of the filters are addressed, with attention given to tunability. Secondly, a concise overview of the active components discussed throughout the review is presented. The third section offers a comprehensive literature review of several outstanding filter proposals, concluding with a summary.

Filter Design Constraints and Classification

An assortment of methods for making voltage and current mode filters utilizing current transports have been examined in [3,5,23-25]. The design of filters presents a multidimensional challenge, making it difficult to fully meet and optimize every aspect, often resulting in compromises among different factors. When designing filters, the following considerations should be considered:

- Utilizing the least number of dynamic and detached components for usage.
- Opting for indistinguishable dynamic components is invaluable as it encourages improved transistor format, especially in profound submicron advances. Utilizing grounded detached components (capacitors and resistors), as they are less demanding to make, involve less chip zone, and appear successful commotion dismissal properties.
- Ensuring the ability to independently regulate the frequency (ω_o), quality factor (Q), bandwidth (B.W.), and gain of the filter. The ability to achieve all five standard filtering responses at the same time without the necessity of changing the structure. Negligible affectability to inactive components and a tall Q figure.
- A moo input impedance coupled with a tall yield impedance comes about in decreased twisting and encourages simple cascading.

There are no restrictions on matching passive components. Based on the design methodology chosen to fulfill the design requirements, filters can be categorized in different ways. A comprehensive classification is provided in Table 1.

One of the most important design criteria for mixed mode systems nowadays is tunability. A wide range of frequency filtering can be achieved with a single filter structure by proper tuning, which also helps to reduce current and voltage offsets created during fabrication, allowing for the creation of filters with exact filtering properties. There are two ways to provide tunability in the filter design. Making the active elements used in the filter implementation adjustable is one strategy [26, 27]. Making the passive components (resistors) employed in the filter implementation adjustable is how the second method operates [28].

Table 1: Classification of Filters.

Design Criterion	Classification
The way input and output currents are coupled to the active devices	Single Input Single Output (SISO), Multi Input Single Output (MISO), Multi Input Multi Output (MIMO)
Type of responses realized	All pass (AP), Band pass (BP), Notch, High pass (HP) and Low pass (LP)
Tunability (type)	Tunable (Via bias current or digital control) or Non-Tunable
Independent control of filter parameters (Q, $\omega_o$and H_o)	Capable or Not capable
Connection of Passive elements to the active blocks.	Grounded or floating
Active elements used in filter implementation	Identical or Distinct
Components Matching requirement	Critical or Independent of matching requirements

The fact that filters that can identify HP, LP, and BP reactions can also be used to identify APand score reactions with a simple expansion of yield streams at the expense of a few additional dynamic components, as shown in Equations (1-2), demonstrates the superiority of the display mode plan.

$$I_{Notch} = I_{HP} + I_{LP}(\mathrm{I_{HP}\ and\ I_{LP}in\ same\ polarity}) \quad (1)$$

$$I_{AP} = I_{HP} + I_{LP} + I_{BP}(\mathrm{I_{BP}\ must\ be\ of\ opposite\ polarity\ compared\ to\ I_{HP}\ and\ I_{LP}}) \quad (2)$$

Evaluate the Current Conveyor and Its alterations:

Since its debut, the CC has gained widespread recognition as the most praised independent current-mode active element. Numerous innovative variations of this device have emerged because of the research focus on it; each one has unique advantages in achieving a specific set of applications. For the readers' comfort, a brief outline of all the numerous current transports utilized in the amalgamation of the filters inspected in this study is given underneath. The most prevalent dynamic square and the central component of most current-mode gadgets is the moment-era current transport. As seen in Figure 1, it comprises a voltage supporter between the Y and X hubs and a current adherent between the X and Z hubs. As seen in Figure 1(a-c), the expansion of current mirrors makes it basic to copy and nullify current, coming about in double yield current transports (DOCCII), positive (CCII+), and negative (CCII-). The lattice Condition 3 gives the V-I relationship of CCII, where ± indicates the sort of CCII, and β and α are the current and voltage exchange proportions, respectively, with perfect values of ±1.

$$\begin{bmatrix} V_X \\ I_Y \\ I_Z \end{bmatrix} = \begin{bmatrix} 0 & \beta & 0 \\ 0 & 0 & 0 \\ \pm\alpha & 0 & 0 \end{bmatrix} \begin{bmatrix} I_X \\ V_Y \\ V_Z \end{bmatrix} \quad (3)$$

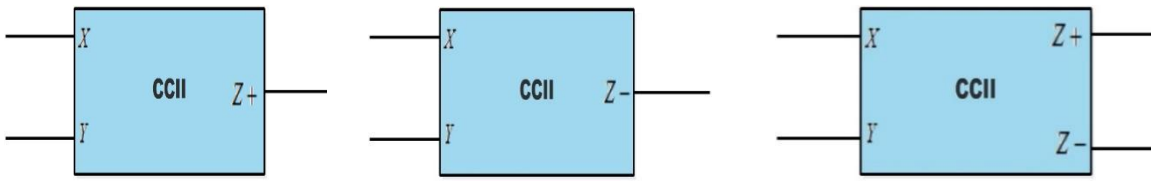

Figure 1:(a) CCII+ (b) CCII- (c) DOCCII.

MOCCII is the general term for a CCII with n output terminals. Equation 4 and Figure 2 provide the block diagram and characteristic equation, respectively. With more output terminals, the features are identical to those of the CCII. The installation of current mirrors does this.

$$\begin{bmatrix} V_X \\ I_Y \\ I_{Z1} \\ \cdot \\ \cdot \\ \vdots \\ I_{Zn} \end{bmatrix} = \begin{bmatrix} 0 & \beta & 0 \\ 0 & 0 & 0 \\ \pm\alpha & 0 & 0 \end{bmatrix} \begin{bmatrix} I_X \\ V_Y \\ V_Z \end{bmatrix} \quad (4)$$

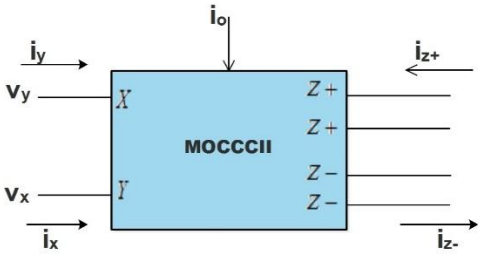

Figure 2: Multi output current conveyor (MOCCII).

The current controlled current transport (CCCII) is another well-known CC. It is comparable to CCII but contains a parasitic resistance at the current input X terminal R_x that may be balanced by inclination current. This characteristic gives the existing transport electronic tunability. Network Condition 5 gives the V-I relationship of CCCII. In Figure 3, the piece graph is appeared. It is to be famous that CCCII with more than two yield terminals will be alluded as MOCCCII.

$$\begin{bmatrix} I_Y \\ V_X \\ I_Z \end{bmatrix} = \begin{bmatrix} 0 & 0 & 0 \\ 1 & R_X & 0 \\ 1 & \pm 1 & 0 \end{bmatrix} \begin{bmatrix} V_Y \\ I_X \\ V_Z \end{bmatrix} \quad (5)$$

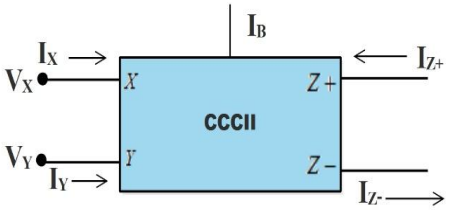

Figure 3: Current controlled current conveyor (CCCII).

Electronically tunable current conveyor (ECCII) is the result of another minor change to CCII. Bias currents are used to adjust the ECCII's output current gain [20]. contains the CMOS implementation. Equation 6 and Figure 4 provide the ECCII's characteristic equation and block diagram, respectively:

$$\begin{bmatrix} I_Y \\ V_X \\ I_{Z1} \end{bmatrix} = \begin{bmatrix} 0 & 0 & 0 \\ 1 & 0 & 0 \\ 0 & \pm k & 0 \end{bmatrix} \begin{bmatrix} V_Y \\ I_X \\ V_Z \end{bmatrix} \quad (6)$$

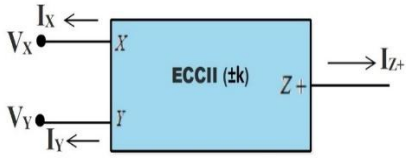

Figure 4: Electronically tunable current conveyor (ECCII).

The sole distinction between the Inverting Current Transport (ICCII) and CCII is the altering voltage exchange characteristics between the Y and X hubs (VY=-VX). Equation 7 and Figure 5 provide the ICCII's characteristic equation and block diagram, respectively

$$\begin{bmatrix} I_Y \\ V_X \\ I_Z \end{bmatrix} = \begin{bmatrix} 0 & 0 & 0 \\ -1 & 0 & 0 \\ 0 & \pm 1 & 0 \end{bmatrix} \begin{bmatrix} V_Y \\ I_X \\ V_Z \end{bmatrix} \quad (7)$$

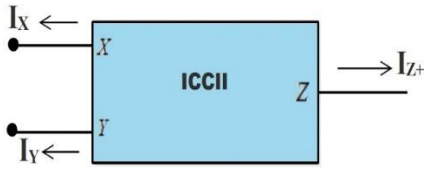

Figure 5: Inverting current conveyor (ICCII).

Another kind of CCII is the dual X current conveyor (DXCCII), which was suggested by Zeki et al. [34]. It might be considered the fusion of ICCII and CCII. It is said to be a flexible block for the implementation of tunable filters. Figure 6 shows that it is a five-terminal device. Equation 8 describes the V-I relation.

$$\begin{bmatrix} I_Y \\ V_{XP} \\ V_{Xn} \\ I_{ZP} \\ I_{Zn} \end{bmatrix} = \begin{bmatrix} 0 & 0 & 0 \\ 1 & 0 & 0 \\ -1 & 0 & 0 \\ 0 & 1 & 0 \\ 0 & 0 & 1 \end{bmatrix} \begin{bmatrix} V_Y \\ I_{XP} \\ I_{Xn} \end{bmatrix} \quad (8)$$

Figure 6: Dual X current conveyor (DXCCII).

As demonstrated in [16], the cascade of CCCII and the OTA comes about in the current-controlled current transport transconductance intensifier (CCCCTA), another imaginative building component. Both legitimate channel and oscillator usage are said to be congruous with this usage. Through their individual inclination streams, the OTA's transconductance and the parasitic resistance at X terminal Rx can be freely directed. In a comparable design, cascading of CCII and the OTA leads to CCTA. In this usage, as it were, the transconductance can be controlled through the predisposition current. The two gadgets are indistinguishable but that the CCCTA has controllable parasitic resistance at the X terminal, whereas the CCTA does not. Equations (9–10) and Figure 7 (a–b) give the CCCCTA's characteristic condition and square chart, separately:

$$\begin{bmatrix} I_Y \\ V_X \\ I_Z \\ I_O \end{bmatrix} = \begin{bmatrix} 0 & 0 & 0 & 0 \\ R_x & 1 & 0 & 0 \\ 1 & 0 & 0 & 0 \\ 0 & 0 & \pm g_m & 0 \end{bmatrix} \begin{bmatrix} I_X \\ V_Y \\ V_Z \\ V_o \end{bmatrix} \quad (9)$$

$$\begin{bmatrix} I_Y \\ V_X \\ I_Z \\ I_O \end{bmatrix} = \begin{bmatrix} 0 & 0 & 0 & 0 \\ 0 & 1 & 0 & 0 \\ 1 & 0 & 0 & 0 \\ 0 & 0 & \pm g_m & 0 \end{bmatrix} \begin{bmatrix} I_X \\ V_Y \\ V_Z \\ V_O \end{bmatrix} \quad (10)$$

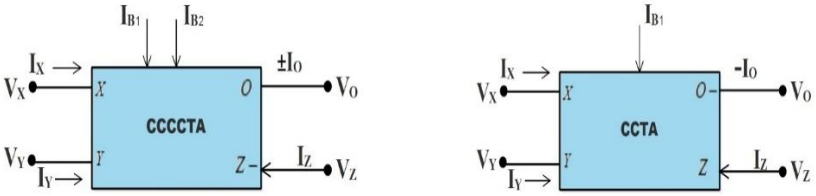

Figure 7: (a) Current controlled current conveyor transconductance amplifier (CCCCTA) (b) Current conveyor transconductance amplifier.

Digitally controlled current follower (DCCF) is another new active element [4]. The circuits carefully controlled pick up work is planned to utilize a current division organize (CDN). The matrix Equation11 describes the circuit:

$$\begin{bmatrix} I_Z \\ V_X \end{bmatrix} = \begin{bmatrix} 0 & \pm\alpha \\ 0 & 0 \end{bmatrix} \quad (11)$$

Where, $\alpha=\sum_{i=1}^{n} d_i 2^{-i}$ is the current gain of DCCF, d_i is the digital bit and *n* is the size of the control bit. Figure 8 displays the DCCF block diagram.

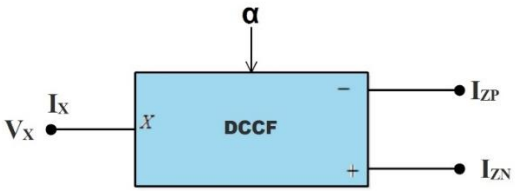

Figure 8: Digitally controlled current follower (DCCF).

In [35], a carefully programmable current transport (DPCC) is presented utilizing the current summing organize (CSN). Carefully programmable current pickup or current constriction comes about from the expansion of the current summation arrange (CSN) to the current transport (CCII). Programmable current constriction happens when the CSN is provided to the current input terminal X, and programmable current pickup happens when the CSN is included in the current yield terminal Z. Figure 8 displays the circuit, while Equation 12's matrix equations illustrate the V-I connection.

$$\begin{bmatrix} I_Y \\ V_X \\ I_Z \end{bmatrix} = \begin{bmatrix} 0 & 0 & 0 \\ 1 & 0 & 0 \\ 0 & K^{\pm m} & 0 \end{bmatrix} \begin{bmatrix} V_Y \\ I_X \\ V_Z \end{bmatrix} \quad (12)$$

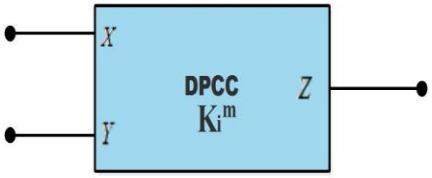

Figure 9: Digitally programmable current conveyor (DPCC).

The brief outline of the active components indicates that CCII serves as their central component. Besides, the components examined can be executed in both bipolar and CMOS innovations, and so the filter characteristics will depend on the inside structures of these dynamic components. Here we are, as it were interested to ponder the different topologies of all-inclusive filters utilizing these dynamic components to get an understanding of current mode filter design.

Universal Filters Review and Classification:

The Universal filters are divided into two groups in this review. Group-1 filters have more than one input, like MISO and MIMO types, and Group-2 filters are of the SIMO type. First the MISO and MIMO filters are reviewed, followed by SIMO.

Multi input single output filters and Multi input multi output filters:

Suwanjan et al. [36] utilized CCCCTA to figure it out a current mode widespread filter showing all standard functions. The CCCCTA, being a combination of CCCII and OTA, has a double tunable property. The MISO sort filter uses two CCCCTA and two grounded capacitors. The filter offers tall yield impedance driving to simple cascading. The filter has the capability of autonomous tuning of frequency and quality figure by means of inclination streams. The realization is given in Figure 10 and the exchange capacities in Conditions (13-15). Table 2 gives the size and grouping of inputs to be connected to realize a specific reaction. Thosdeekoraphat et al. proposed another CCTA-based execution [37]. As seen in Figure 11, the MISO sort filter is ideal for IC use because it consists of two CCTAs and two grounded capacitors. LP, HP, BP, BR, and AP reactions can all be realized using the filter structure. In this implementation, the inactive resistors are replaced by the OTA's

transconductance. Predisposition current allows for the electronic tuning of the filter settings. Conditions (16–23) provide the channel exchange capacities, Q, and ω_0. The intensity and grouping of inputs to be coupled in order to achieve a particular reaction are shown in Table 3.

$$I_{Out} = \mathrm{k}\left(\frac{I_{in2}S^2\frac{C_1C_2R_{x1}}{g_{m2}} + I_{in1}\frac{sC_2}{g_{m2}} + I_{in3}}{S^2\frac{C_1C_2R_{x1}}{g_{m2}} + \frac{sC_2k}{g_{m2}} + 1}\right) \tag{13}$$

$$\omega_o = \sqrt{\frac{g_{m2}}{C_1C_2\,R_{x1}}} \tag{14}$$

$$Q = \frac{1}{k\sqrt{\frac{C_1R_{x1}g_{m2}}{C_2}}} \tag{15}$$

Table 2: Filter input excitation sequence.

Filter Responses	Input Selections		
I_{Out}	I_{in1}	I_{in2}	I_{in3}
I_{LP}	0	0	I_{in}
I_{HP}	0	I_{in}	0
I_{BP}	I_{in}	0	0
I_{BR}	0	I_{in}	I_{in}
I_{AP}	-I_{in}	I_{in}	I_{in}

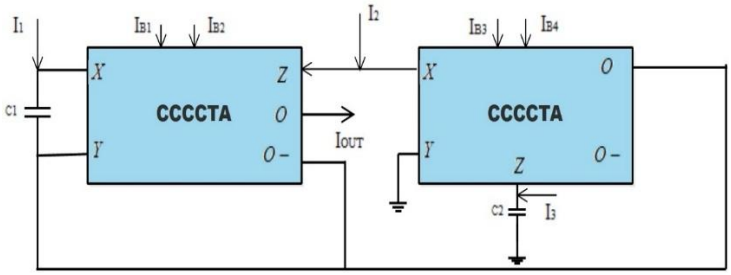

Figure 10: CCCCTA based filter topology [36].

$$I_{Out} = \frac{\left(S^2 + \frac{g_{m1}}{C_1}s + {g_{m1}g_{m2}}/{C_1C_2}\right)I_{in3} - \left({g_{m1}g_{m2}}/{C_1C_2}\right)I_{in2} - \frac{g_{m1}}{C_1}I_{in1}}{S^2 + \frac{g_{m1}}{C_1}s + {g_{m1}g_{m2}}/{C_1C_2}} \tag{16}$$

$$I_{LP} = -\frac{{g_{m1}g_{m2}}/{C_1C_2}}{S^2 + \frac{g_{m1}}{C_1}s + \frac{g_{m1}g_{m2}}{C_1C_2}} \tag{17}$$

$$I_{HP} = \frac{S^2}{S^2 + \frac{g_{m1}}{C_1}s + \frac{g_{m1}g_{m2}}{C_1C_2}} \tag{18}$$

$$I_{BR} = -\frac{S^2 + \frac{g_{m1}g_{m2}}{C_1C_2}}{S^2 + \frac{g_{m1}}{C_1}s + \frac{g_{m1}g_{m2}}{C_1C_2}} \tag{19}$$

$$I_{BP} = -\frac{{g_{m1}}/{C_1}}{S^2 + \frac{g_{m1}}{C_1}s + \frac{g_{m1}g_{m2}}{C_1C_2}} \tag{20}$$

$$I_{AP} = \frac{S^2 - \frac{g_{m1}}{C_1} + \frac{g_{m1}g_{m2}}{C_1C_2}}{S^2 + \frac{g_{m1}}{C_1}s + \frac{g_{m1}g_{m2}}{C_1C_2}} \tag{21}$$

$$Q = \sqrt{\frac{g_{m2}C_1}{g_{m1}C_2}} \tag{22}$$

$$\omega_o = \sqrt{\frac{g_{m1}g_{m2}}{C_1C_2}} \tag{23}$$

Table 3: Filter input excitation sequence.

Filter Responses	Input Selections		
	I_{in1}	I_{in2}	I_{in3}
I_{LP}	0	1	0
I_{HP}	1	1	1
I_{BP}	1	0	0
I_{BR}	1	0	1
I_{AP}	2	0	1

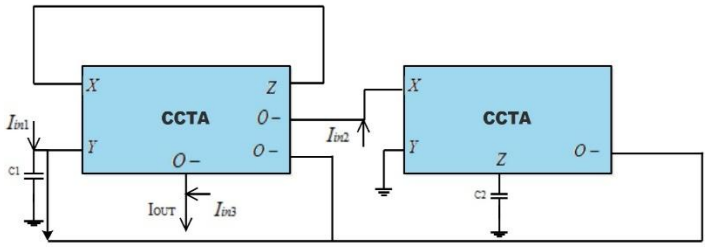

Figure 11: CCTA based filter topology [37].

Chen et al. [38] proposed a current mode biquadratic filter that, depending on how inputs are connected to the channel, can realize HP, LP, BR, BP, and AP reactions at the same time. Three multi-output ICCII, three grounded resistors, and two grounded capacitors constitute the MIMO sort filter. Since of its tall yield impedance and need of component coordinating prerequisites, the filter has great cascade ability. Figure 12 outlines how the filter is actualized. Conditions (24–29) provide the filter exchange capacities as well as reverberation recurrence and quality calculation equations. Furthermore, the filters Q and ωo can be balanced orthogonally. The input grouping and coordinating filter reactions appear in Table 4.

$$I_{O1} = \frac{-(S^2C_1C_2 + G_2G_3)I_{i1} + sC_2G_1I_{i2}}{S^2C_1C_2 + sC_2G_1 + G_2G_3} \tag{24}$$

$$I_{O2} = \frac{sC_2G_2I_{i1} + sC_2G_2I_{i2}}{S^2C_1C_2 + sC_2G_1 + G_2G_3} \tag{25}$$

$$I_{O3} = \frac{G_2G_3I_{i1} - (S^2C_1C_2 + sC_2G_1)I_{i2}}{S^2C_1C_2 + sC_2G_1 + G_2G_3} \tag{26}$$

$$I_{O4} = \frac{-S^2C_1C_2I_{i1} - S^2C_1C_2I_{i2}}{S^2C_1C_2 + sC_2G_1 + G_2G_3} \tag{27}$$

$$\omega_o = \sqrt{\frac{1}{C_1C_2\,R_2R_3}} \tag{28}$$

$$Q = R_1\sqrt{\frac{C_1}{C_2R_2R_3}} \tag{29}$$

Table 4: Filter input excitation sequence

Filter Responses	Input Selections	
	Ii_1	Ii_2
I_{LP} (inverting)	I_{in}	0
I_{BP} (non-inverting)	I_{in}	0
I_{HP} (inverting)	I_{in}	0
I_{BS} (inverting)	I_{in}	0
I_{AP} (inverting)	I_{in}	I_{in}

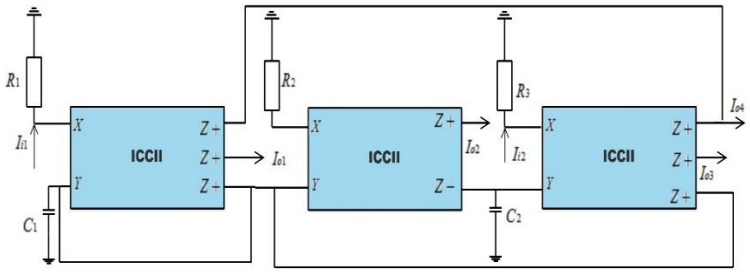

Figure 12: ICCII based filter topology [38].

A flexible MISO sort current mode all inclusive filter utilizing two MOCCCII and two grounded capacitors was displayed by Channumsin et al. [39]. Figure 13 shows the MISO filter which does not require component matching and can recognize all the conventional responses (HP, LP, BR, BP, and AP). The filter can independently regulate its bandwidth and ω_o, and it contains all high impedance output nodes for simple cascading. Equations (30–33) provide the filter's transfer function, while Table 5 provides the filter excitation sequence.

$$I_o = \frac{(s^2R_{x1}R_{x2}C_1C_2 + sR_{x2}C_2 + 1)I_1 + (sR_{x2}C_2)(I_2 + I_3) + I_4}{(s^2R_{x1}R_{x2}C_1C_2 + sR_{x2}C_2 + 1)} \tag{30}$$

$$\omega_o = {1}\Big/{\sqrt{R_{x1}R_{x2}C_1C_2}} \tag{31}$$

$$Q = \sqrt{\frac{R_{x1}C_1}{R_{x2}C_2}} \tag{32}$$

$$\text{B.W.} = \frac{1}{R_{x1}C_1} \tag{33}$$

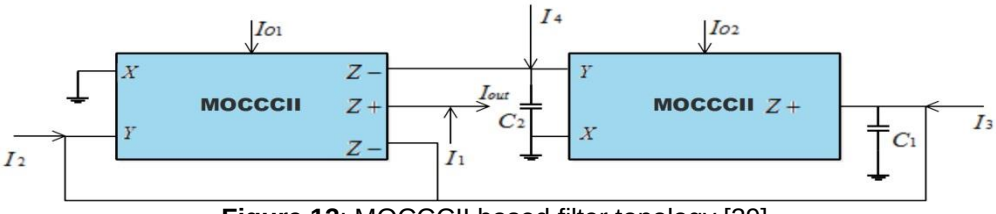

Figure 13: MOCCCII based filter topology [39].

Table 5: Filter input excitation sequence

Filter Responses	Input Selections			
	I_1	I_2	I_3	I_4
I_{LP}	0	0	0	I_{in}
I_{BP}	0	0	I_{in}	0
I_{HP}	I_{in}	0	$-I_{in}$	$-I_{in}$
I_{BS}	I_{in}	0	$-I_{in}$	0
I_{AP}	I_{in}	$-I_{in}$	$-I_{in}$	0

Tangsrirat et al. [40] give a tunable filter based on DOCCCII that can recognize both altering and non-inverting sort BP and LP reactions in expansion to HP and AP. Three DOCCCII and two grounded capacitors make up the circuit. Due to its MIMO plan, the circuit is incapable of performing all its operations at once. Moreover, cascading with taking after stages is made straightforward by the tall impedance yields. The circuit, moreover, did not show any component coordinating confinement. The circuit schematic appears in Figure 14. The filter exchange capacities along with B.W. and ω_0 are given in Conditions (34-39). The channel recurrence and transmission capacity can be tuned through predisposition current. The filter excitation grouping is given in Table 6.

$$\mathrm{I}_{oA} = \frac{(s^2 R_{x1} R_{x2} C_1 C_2 + s R_{x2} C_2 + 1) I_1}{(s^2 R_{x1} R_{x2} C_1 C_2 + s R_{x2} C_2 + 1)} \tag{34}$$

$$\mathrm{I}_{oB} = -\frac{s R_{x2} C_2 (I_1 - I_2)}{(s^2 R_{x1} R_{x2} C_1 C_2 + s R_{x2} C_2 + 1)} \tag{35}$$

$$\mathrm{I}_{oC} = -\frac{(I_1 - I_2)}{(s^2 R_{x1} R_{x2} C_1 C_2 + s R_{x2} C_2 + 1)} \tag{36}$$

$$\omega_o = \sqrt{\frac{1}{R_{x1} R_{x2} C_1 C_2}} \tag{37}$$

$$\mathrm{B.W.} = \frac{1}{R_{x1} C_1} \tag{38}$$

$$Q = \sqrt{\frac{R_{x1} C_1}{R_{x2} C_2}} \tag{39}$$

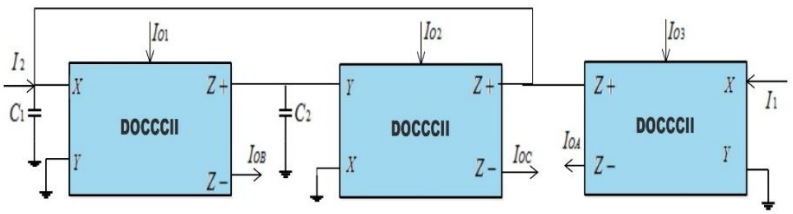

Figure 14: DOCCCII based filter topology [40].

Three MISO type biquadratic universal filter architectures were presented by Horng et al. [41] to realize all five conventional filter responses. All the filters had high output impedance, no component matching requirements, and three multi output current conveyors (MOCCII). Two grounded capacitors and one coasting resistor were utilized in the beginning development. It had orthogonal control over recurrence and quality figure.

Table 6: Filter input excitation sequence.

Filter Responses	Input Selections		Output node
	I_1	I_2	
I_{LP}	0	I_{in}	I_{oC}
I_{BP}	0	I_{in}	I_{oB}
I_{HP}	I_{in}	0	$I_{oA} + I_{oB} + I_{oC}$
I_{BS}	I_{in}	0	$I_{oA} + I_{oB}$
I_{AP}	I_{in}	-I_{in}	$I_{oA} + I_{oB}$

Two grounded capacitors, one drifting resistor, and one grounded resistor were utilized in the moment filter. Q and "ω"0 might not be freely controlled. Three grounded resistors and one capacitor were used in the final structure. It was ideal for the implementation of IC. Equations (40–44) and Figure 15 (a–c) provide the filter architectures and their distinctive transfer functions. The filter excitation sequence is presented in Table 7.

$$I_{out} = \frac{S^2C_1C_2G_3I_{in3} + sC_2G_2G_3I_{in2} - G_1G_2G_3I_{1n1} + (S^2C_1C_2G_3 + G_1G_2G_3)I_{in4} + (s^2C_1C_2G_3 - sC_2G_1G_2 + G_1G_2G_3)I_{in5}}{S^2C_1C_2G_3 + sC_2G_1G_2 + G_1G_2G_3} \quad (40)$$

$$I_{out} = \frac{S^2C_1C_2I_{in3} - sC_2G_2I_{in2} - G_1G_2I_{1n1} + (S^2C_1C_2 + G_1G_2)I_{in4} + (s^2C_1C_2 - sC_2G_2 + G_1G_2)I_{in5}}{S^2C_1C_2 + sC_2G_2 + G_1G_2} \quad (41)$$

$$I_{out} = \frac{-S^2C_1C_2I_{in3} + sC_1G_1I_{in2} + G_1G_2I_{1n1} - (S^2C_1C_2 + G_1G_2)I_{in4} + (s^2C_1C_2 - sC_1G_1 + G_1G_2)I_{in5}}{S^2C_1C_2 + sC_1G_1 + G_1G_2} \quad (42)$$

$$\omega_o = \sqrt{\frac{G_1G_2}{C_1C_2}} \quad (43)$$

$$Q = \sqrt{\frac{C_2G_2}{C_1G_1}} \quad (44)$$

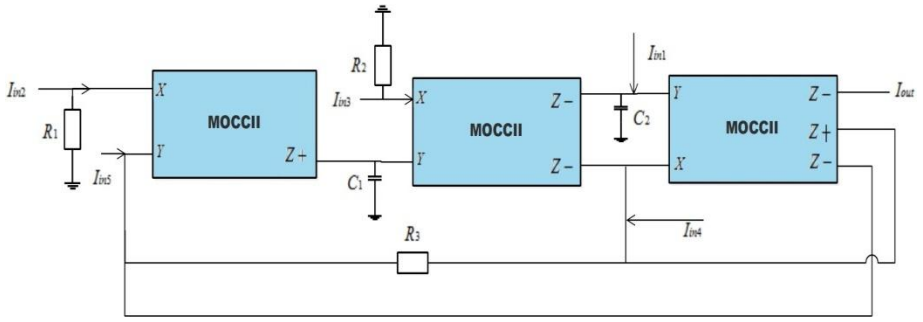

(a)

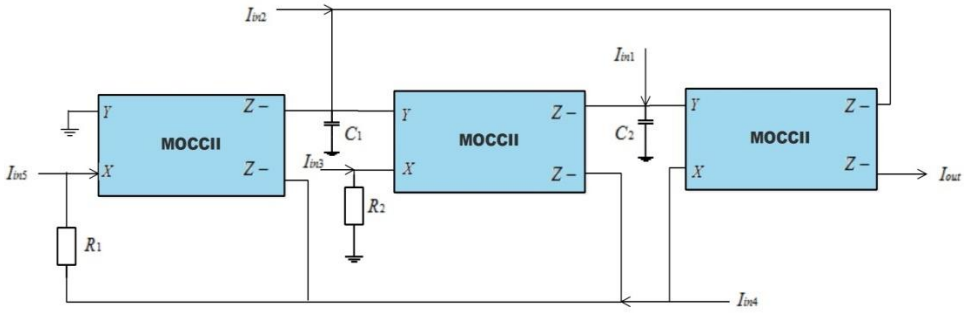

(b)

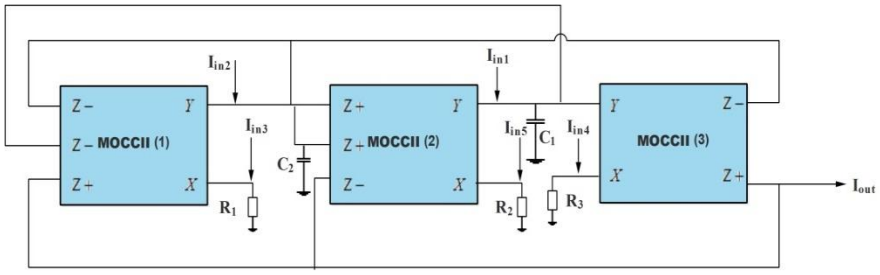

(c)

Figure 15: MOCCII based filter topology (a) Structure 1 (b) Structure 2 (c) Structure 3 [41].

Table 7: Filter input excitation sequence.

Filter Responses	Input Selections				
	I_1	I_2	I_3	I_4	I_5
I_{LP}	I_{in}	0	0	0	0
I_{BP}	0	I_{in}	0	0	0
I_{HP}	0	0	I_{in}	0	0
I_{NOTCH}	0	0	0	I_{in}	0
I_{AP}	0	0	0	0	I_{in}

Horng et al. propose a biquadratic current mode filter [42]. The sort of filter is MISO. Three ICCII, two grounded capacitors, one grounded resistor, and one drifting resistor are utilized in the filter. LP, HP, BP, notch, and AP responses can all be produced by the circuit. There are no components in the circuit that meet the requirements. Easy cascading is made possible by the output's availability at the high impedance node. Additionally, the circuit doesn't need additional current followers to replicate input current for the implementation of AP and notch responses. The circuit's primary flaw is that not all of the filters can be realized at once. Moreover, frequency and quality factor cannot be adjusted separately. Figure 16 and Equations (45–47) provide the filter schematic and transfer function. Table 8 provides the filter excitation sequence.

$$I_{out} = \frac{S^2C_1C_2(I_{in3} + I_{in4} + I_{in5}) + sG_1C_2(I_{in2} - I_{in5}) + G_1G_2(I_{in1} + I_{in4} + I_{1n5})}{S^2C_1C_2 + sC_2G_1 + G_1G_2} \quad (45)$$

$$\omega_o = \sqrt{\frac{G_1G_2}{C_1C_2}} \quad (46)$$

$$Q = \sqrt{\frac{G_2C_1}{G_1C_2}} \quad (47)$$

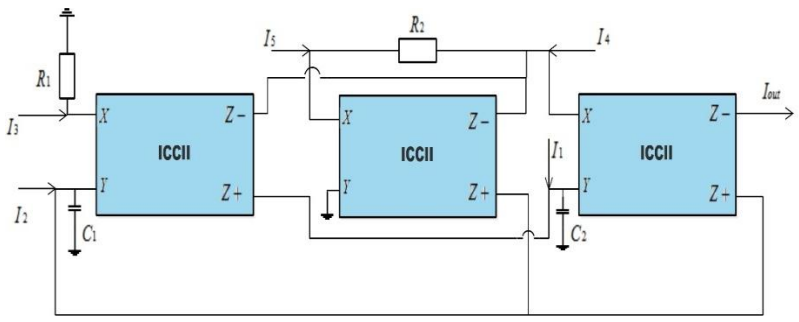

Figure 16: ICCII based filter topology [42].

Table 8: Filter input excitation sequence.

Filter Responses	Input Selections				
	I_1	I_2	I_3	I_4	I_5
I_{LP}	I_{in}	0	0	0	0
I_{BP}	0	I_{in}	0	0	0
I_{HP}	0	0	I_{in}	0	0
I_{NOTCH}	0	0	0	I_{in}	0
I_{AP}	0	0	0	0	I_{in}

An electronically tunable filter utilizing MOCCCII is proposed by Chen et al. [43]. Three MOCCCII and two grounded capacitors were used in the implementation. Without changing its topology, the circuit can be used as a SIMO or MISO filter. Additionally, the frequency, transfer speed, and quality calculations can be adjusted electronically. The circuit has no components that meet the limitations and high impedance output terminals. The circuit schematic is shown in Figure 17. The current transfer functions derived from the circuit analysis are shown in equations (48–50).

$$\frac{I_{01}}{I_{in}} = \frac{-(sC_2G_{x2})I_{i1} - (sC_2G_{x2})I_{i2} - (G_{x2}G_{x3})I_{i3}}{S^2C_1C_2 + sC_2G_{x2} + G_{x2}G_{x3}} \tag{48}$$

$$\frac{I_{02}}{I_{in}} = \frac{-(G_{x2}G_{x3})I_{i1} - (G_{x2}G_{x3})I_{i2} + (sC_1G_{x3} + G_{x2}G_{x3})I_{i3}}{S^2C_1C_2 + sC_2G_{x2} + G_{x2}G_{x3}} \tag{49}$$

$$\frac{I_{03}}{I_{in}} = \frac{(S^2C_1C_2 + G_{x2}G_{x3})I_{i1} - (sC_2G_{x2})I_{i2} - (G_{x2}G_{x3})I_{i3}}{S^2C_1C_2 + sC_2G_{x2} + G_{x2}G_{x3}} \tag{50}$$

The filter's operation is determined on the input current value. When I_{i2}=I_{i3}=0 and I_{i1}=I_{in} The filter will operate similarly to a SIMO filter. The output currents I_{01},$I_{02}$and I_{03} will acknowledge the responses of the non-inverting BR filter, inverting LP, and inverting BP filters. Moreover, non-inverting HP can be obtained by adding the I_{02} and I_{03} and AP can be obtained by connecting I_{01} and I_{03}. The filter can work in MISO arrangement with yield harbour I_03 when left agreeing to grouping given in Table 9.

Table 9: Input application sequence

Filter Responses	Input Selections		
	I_{i1}	I_{i2}	I_{i3}
I_{LP}	0	0	aI_{in}
I_{BP}	0	I_{in}	0
I_{HP}	I_{in}	0	I_{in}
I_{BR}	I_{in}	0	0
I_{AP}	I_{in}	I_{in}	0

Equations (51–53) provide the resonance frequency, which is the same for both modes of operation. The filters' three parameters can all be changed electrically.

$$\omega_o = \sqrt{\frac{G_{x2}G_{x3}}{C_1C_2}} \tag{51}$$

$$Q = \sqrt{\frac{C_1G_{x3}}{C_2G_{x2}}} \tag{52}$$

$$\text{B.W.} = \frac{G_{x2}}{C_1} \tag{53}$$

Because there are high impedance outputs available, the filter can be cascaded quickly and is free of components that match condition.

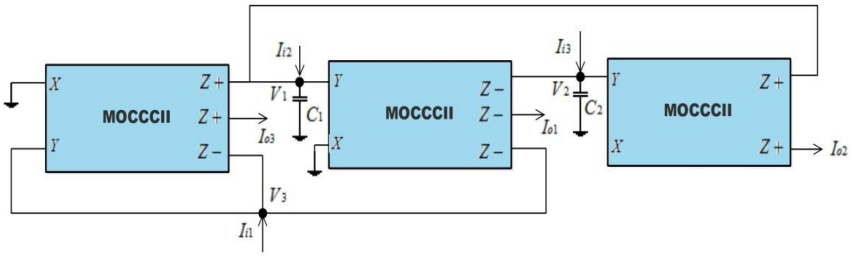

Figure 17: MOCCCII based filter topology [43].

Single input multi output filters:

A non-ideal shunt RL circuit-based all-inclusive filter was demonstrated by Fabre et al. [44]. Two extra sort CCIIs, two grounded capacitors, one drifting resistor, and one grounded resistor make up the circuit. HP, LP, and BP reactions were displayed by the filter. The circuit's main feature is that its dynamic and passive sensitivities are independent of the Q calculation. According to Figure 18's filter designs, the yield is open at the moo impedance hubs, causing botches during cascading. If tall impedance is needed, MOCCII can be used to obtain the LP and BP reactions at tall impedance Z terminals. With the broad filter, Q and ω_0 can be freely adjusted. The filter transfer functions are given in equations (58).

$$\frac{I_{LP}}{I_{IN}} = -\frac{1}{1 + R_2C_2S + R_1R_2C_2C_1S^2} \tag{54}$$

$$\frac{I_{BP}}{I_{IN}} = -\frac{R_2C_2S}{1 + R_2C_2S + R_1R_2C_2C_1S^2} \tag{55}$$

$$\frac{I_{HP}}{I_{IN}} = +\frac{R_1R_2C_2C_1S^2}{1 + R_2C_2S + R_1R_2C_2C_1S^2} \tag{56}$$

$$\omega_o = \sqrt{\frac{1}{R_1R_2C_1C_2}} \tag{57}$$

$$Q = \sqrt{\frac{R_1C_1}{R_2C_2}} \tag{58}$$

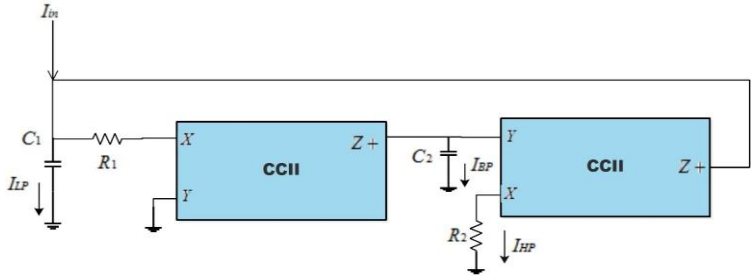

Figure 18: CCII based filter topology [44].

Bhaskar et al. [45] demonstrated a filter based on negative current transports that could simultaneously realize all the common filter capabilities (LP, HP, BP, and BR). The filter, in effect, uses two CCIIs, two grounded capacitors, one drifting resistor, and one grounded resistor. The filter shown in Figure 19 emphasizes the quality figure tunability, autonomous transmission capacity, and lack of coordination-limiting components. Q and ω_0, the filter transfer functions, are given by equations (59–64). Senani et al. [46] proposed an effective filter construction using only three MOCCII. The filter can produce HP, LP, and BP responses. It can also synthesis AP and notch responses using additional active elements. The frequency, Q, and gain can all be independently adjusted by the filter. The

architecture depicted in Figure 20 is a good option for IC implementation because it uses two capacitors and four resistors, all of which are grounded. Equations (65-73) provide the filter transfer functions, Q, and ω_0.

$$T_{LP} = \frac{{}^{1}/_{(R_1R_2C_1C_2)}}{S^2 + S/R_2C_2 + 1/R_1R_2C_1C_2} \tag{59}$$

$$T_{BP} = \frac{{}^{S}/_{(R_2C_2)}}{S^2 + S/R_2C_2 + 1/R_1R_2C_1C_2} \tag{60}$$

$$T_{BR} = \frac{S^2 + {}^{1}/_{(R_1R_2C_1C_2)}}{S^2 + S/R_2C_2 + 1/R_1R_2C_1C_2} \tag{61}$$

$$\omega_o = \sqrt{\frac{1}{R_1R_2C_1C_2}} \tag{62}$$

$$Q = \sqrt{\frac{R_2C_2}{R_1C_1}} \tag{63}$$

$$\text{B.W.} = \frac{1}{R_2C_2} \tag{64}$$

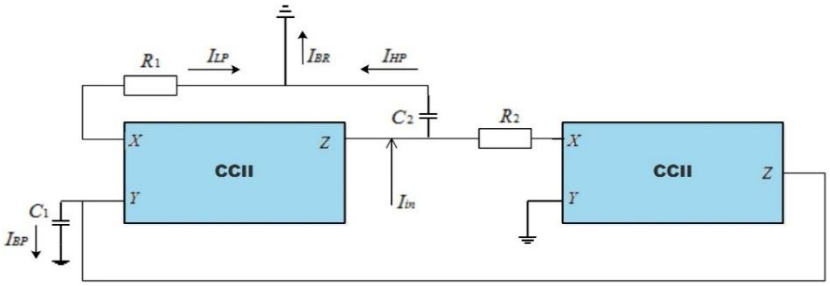

Figure 19: CCII based filter topology [45].

$$\frac{\mathrm{I}_{01}}{\mathrm{I}_{IN}} = \frac{\left({}^{R_3}/_{R_4}\right)S^2}{S^2 + S(1/R_1C_1) + 1/R_1R_2C_1C_2} \tag{65}$$

$$\frac{\mathrm{I}_{02}}{\mathrm{I}_{IN}} = \frac{\left({}^{R_3}/_{R_4}\right)S}{S^2 + S(1/R_1C_1) + 1/R_1R_2C_1C_2} \tag{66}$$

$$\frac{\mathrm{I}_{03}}{\mathrm{I}_{IN}} = \frac{\left({}^{R_3}/_{R_4}\right)\left(\frac{1}{R_1R_2C_1C_2}\right)}{S^2 + S(1/R_1C_1) + 1/R_1R_2C_1C_2} \tag{67}$$

$$\frac{\mathrm{I}_{04}}{\mathrm{I}_{IN}} = \frac{\left({}^{R_3}/_{R_4}\right)\left(S^2 + \frac{1}{R_1R_2C_1C_2}\right)}{S^2 + S(1/R_1C_1) + 1/R_1R_2C_1C_2} \tag{68}$$

$$\frac{\mathrm{I}_{05}}{\mathrm{I}_{IN}} = \frac{\left({}^{R_3}/_{R_4}\right)\left(S^2 - (1/R_1C_1) + \frac{1}{R_1R_2C_1C_2}\right)}{S^2 + S(1/R_1C_1) + 1/R_1R_2C_1C_2} \tag{69}$$

$$\omega_o = \sqrt{\frac{1}{R_1R_2C_1C_2}} \tag{70}$$

$$\text{B.W.} = \frac{1}{R_1 C_1} \tag{71}$$

$$H_o = {R_3}/{R_4} \tag{72}$$

$$Q = \sqrt{\frac{R_2 C_2}{R_1 C_1}} \tag{73}$$

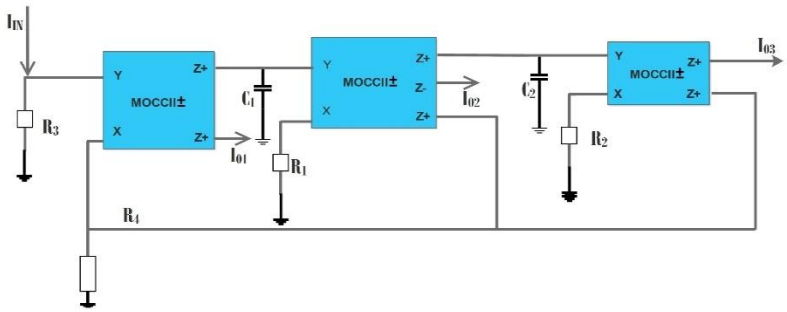

Figure 20: MOCCII based filter topology [46]

ECCII is a new current mode element that was proposed by Minaei et al. [47]. By altering the ratio of the bias currents, the current gain between the ECCII's X and Z terminals can be managed. A present mode universal filter that can recognize (HP, LP, and BP) answers was created using this ECCII. The filter used three ECCII, two grounded capacitors, and two coasting resistors, as appeared in Figure 21. The most eminent angle was the capacity to independently alter the LP filter's pick up. The proposed structure did not make full utilize of ECCII's tunability and has constrained tunability. It is to be famous here that by creating unused inventive structures for channel usage more up to date topologies showing tunable recurrence reaction and quality calculate can be accomplished hence taking full advantage of ECCII. Equations 74 to 78 give the channel exchange capacities, Q, and ω_0. The tunable gains of the corresponding ECCIIs are represented by k(1-3). Five more CCCII-based universal filters were published by the same author [48], giving all the commonplace answers (HP, LP, and BP). The arrangement delineated in Figure 22 utilized parasitic resistance at hub X of the CCCII and as it were utilized two grounded capacitors. The yield current is given at the tall impedance hub, permitting for straightforward cascading, and the recurrence and quality calculate can be independently controlled through predisposition current. The utilize of as well numerous dynamic fixings is the fundamental drawback. Equations 79 to 84 give the channel exchange capacities and ω_0.

$$\frac{\mathrm{I}_{LP}}{\mathrm{I}_{IN}} = \frac{\left({k_3 k_1}/{R_1 R_2 C_1 C_2}\right)}{S^2 + S(1/R_1 C_1) + (k_2 k_1 / R_1 R_2 C_1 C_2)} \tag{74}$$

$$\frac{\mathrm{I}_{HP}}{\mathrm{I}_{IN}} = \frac{(S^2)}{S^2 + S(1/R_1 C_1) + (k_2 k_1 / R_1 R_2 C_1 C_2)} \tag{75}$$

$$\frac{\mathrm{I}_{BP}}{\mathrm{I}_{IN}} = \frac{-s\left({k_1}/{R_1 C_1}\right)}{S^2 + S(1/R_1 C_1) + (k_2 k_1 / R_1 R_2 C_1 C_2)} \tag{76}$$

$$\omega_o = \sqrt{\frac{k_2 k_1}{R_1 R_2 C_1 C_2}} \tag{77}$$

$$Q = \sqrt{\frac{k_2 k_1 R_1 C_1}{R_2 C_2}} \tag{78}$$

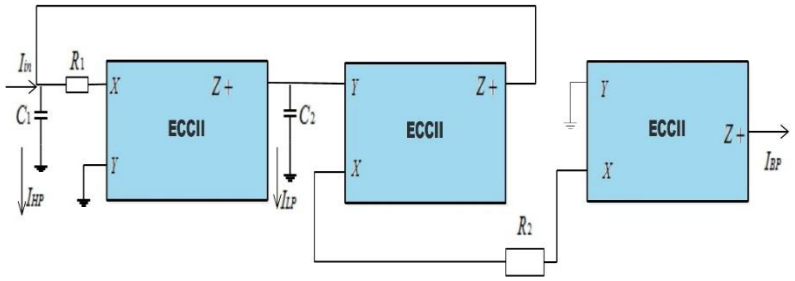

Figure 21: ECCII based filter topology proposed in [47]

$$\frac{\mathrm{I}_{LP}}{\mathrm{I}_{IN}} = \frac{\left(\alpha_3\alpha_1/R_{x1}C_1C_2(R_{x2}+R_{x3})\right)}{D(S)} \tag{79}$$

$$\frac{\mathrm{I}_{BP}}{\mathrm{I}_{IN}} = -\frac{S\left(\frac{\alpha_4}{R_{x4}C_1}\right)}{D(S)} \tag{80}$$

$$\frac{\mathrm{I}_{HP}}{\mathrm{I}_{IN}} = \frac{-S^2(\alpha_5C_3/C_1)}{D(S)} \tag{81}$$

$$D(S) = S^2 + S(R_{x1}+R_{x4}/R_{x1}R_{x4}C_1) + \alpha_2\alpha_1/R_{x1}C_1C_2(R_{x2}+R_{x3}) \tag{82}$$

$$\omega_o = \sqrt{\frac{\alpha_2\alpha_1}{R_{x1}C_1C_2(R_{x2}+R_{x3})}} \tag{83}$$

$$Q = \frac{1}{(C_1+1)}\sqrt{\frac{\alpha_2\alpha_1C_1R_{x4}}{R_{x1}C_2(R_{x2}+R_{x3})}} \tag{84}$$

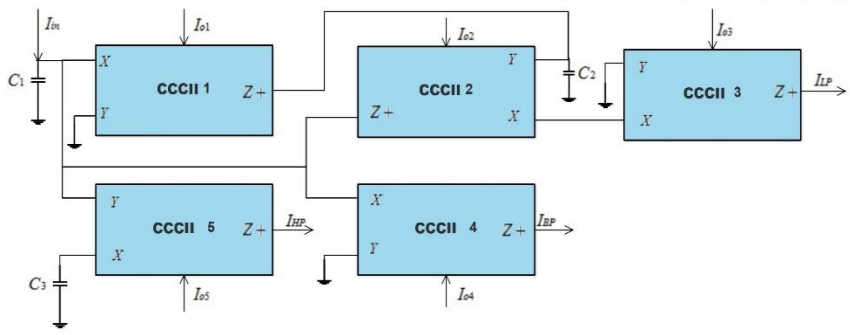

Figure 22: CCCII based filter topology [48]

One double output CCII (DOCCII), two double output OTAs, one single output OTA, and two grounded capacitors make up the widespread filter that Biolek et al. [49] recommended. The execution was engaging for IC execution due to the utilization of grounded detached parts. All five of the customary sifting capacities can be realized by the SIMO sort filter that appears in Figure 23. Notwithstanding the quality calculation, the circuit has the capacity to tune the post-recurrence. Through the utilization of predisposition current, the OTA's transconductance can be modified to modify the post recurrence. There are no confinements on component coordinating. Conditions (85-91) deliver the filter exchange capacities along with Q and ω_0.

$$\frac{\mathrm{I}_{BP}}{\mathrm{I}_{IN}} = \frac{-SC_2g_m}{S^2C_1C_2 + sC_2g_m + g^2{}_m} \tag{85}$$

$$\frac{\mathrm{I}_{HP}}{\mathrm{I}_{IN}} = \frac{S^2C_1C_2}{S^2C_1C_2 + sC_2g_m + g^2{}_m} \tag{86}$$

$$\frac{I_{LP}}{I_{IN}} = \frac{g^2{}_m}{S^2C_1C_2 + sC_2g_m + g^2{}_m} \tag{87}$$

$$\frac{I_{BS}}{I_{IN}} = \frac{S^2C_1C_2 + g^2{}_m}{S^2C_1C_2 + sC_2g_m + g^2{}_m} \tag{88}$$

$$\frac{I_{AP}}{I_{IN}} = \frac{S^2C_1C_2 - SC_2g_m + g^2{}_m}{S^2C_1C_2 + sC_2g_m + g^2{}_m} \tag{89}$$

$$\omega_o = g_m\sqrt{\frac{1}{C_1C_2}} \tag{90}$$

$$Q = \sqrt{\frac{C_1}{C_2}} \tag{91}$$

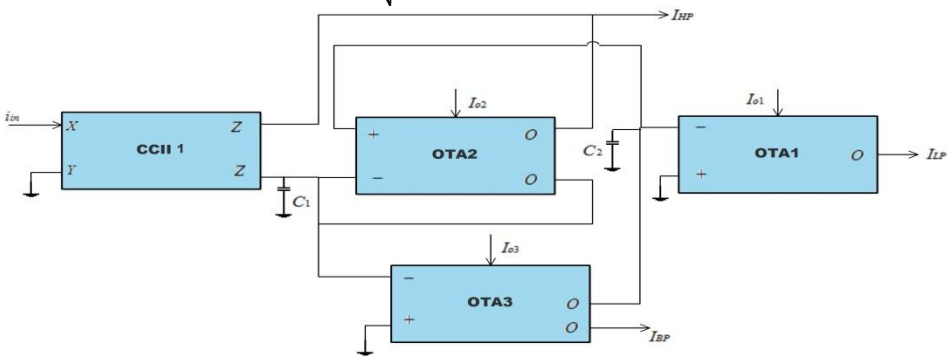

Figure 23: CCII and OTA based filter topology proposed in [49]

A current mode universal filter was introduced by Ozoguz et al. [50]. The simulation of lossy inductance serves as the foundation for the filter topology. Four CCIIs, two resistors, and two floating capacitors make up the circuit seen in Figure 24. While the other two CCIIs produced high impedance output currents, the first two CCIIs simulated lossy inductance. Keep in intellect that whereas an AP reaction can be gotten by rearranging the output current of the moment CCII and including all of its outputs, a indent reaction can moreover be accomplished by combining the output streams of the to begin with and third CCII. There are no component coordinating. The main flaw is that its practical implementation is hampered by the employment of all floating type passive parts. The resonance frequency ωo expression and filter transfer functions are provided in

$$\frac{I_{01}}{I_{IN}} = \frac{-S^2}{S^2 + S(1/R_1C_1) + 1/R_1R_2C_1C_2} \tag{92}$$

$$\frac{I_{02}}{I_{IN}} = \frac{-\left(1/R_1C_1\right)S}{S^2 + S(1/R_1C_1) + 1/R_1R_2C_1C_2} \tag{93}$$

$$\frac{I_{03}}{I_{IN}} = \frac{\left(\frac{-1}{R_1R_2C_1C_2}\right)}{S^2 + S(1/R_1C_1) + 1/R_1R_2C_1C_2} \tag{94}$$

$$\omega_o = \sqrt{\frac{1}{R_1R_2C_1C_2}} \tag{95}$$

$$Q = \sqrt{\frac{R_1 C_1}{R_2 C_2}} \tag{96}$$

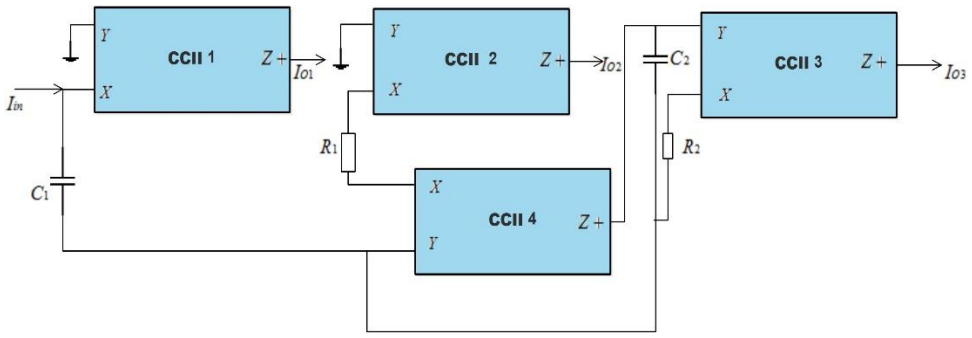

Figure 24: CCII based filter topology [50].

By using a single-output CCII, Chang et al. [51] suggested a universal filter. As seen in Figure 25, he used seven CCIIs, eight resistors, and two capacitors. Every passive component is grounded. In addition to getting LP, BP, and HP reactions, the circuit may also achieve AP and score reactions with the incorporation of reasonable output streams. Tall impedance hubs provide all outputs, simplifying the cascading process. Equations 97 to 101 give the filter exchange capacities and reverberation recurrence, and quality calculate equations.

$$\frac{\mathrm{I}_{HP}}{\mathrm{I}_{IN}} = \frac{S^2 R/R_5}{S^2 + \frac{R}{C_1 R_1 R_4} s + \frac{R}{C_1 C_2 R_1 R_2 R_3}} \tag{97}$$

$$\frac{\mathrm{I}_{LP}}{\mathrm{I}_{IN}} = \frac{\frac{R}{C_1 C_2 R_1 R_2 R_7}}{S^2 + \frac{R}{C_1 R_1 R_4} s + \frac{R}{C_1 C_2 R_1 R_2 R_3}} \tag{98}$$

$$\frac{\mathrm{I}_{BP}}{\mathrm{I}_{IN}} = \frac{-\frac{SR}{C_1 R_1 R_6}}{S^2 + \frac{R}{C_1 R_1 R_4} s + \frac{R}{C_1 C_2 R_1 R_2 R_3}} \tag{99}$$

$$\omega_o = \sqrt{\frac{R}{C_1 C_2 R_1 R_2 R_3}} \tag{100}$$

$$Q = R_4 \sqrt{\frac{C_1 R_1}{C_2 R R_2 R_3}} \tag{101}$$

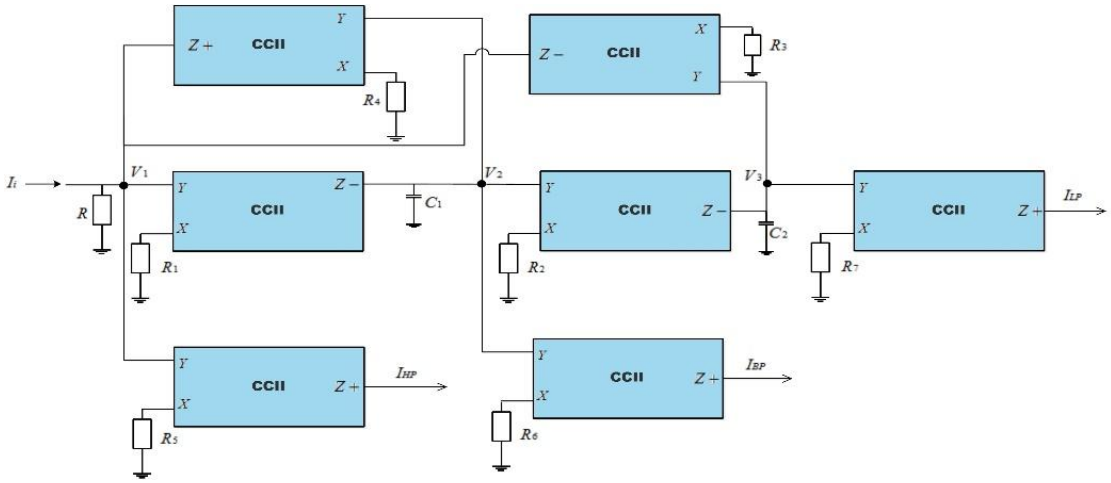

Figure 25: CCII based filter topology [51].

Siripongdee et al. [52] presented a current mode all-inclusive biquadratic filter based on parallel dynamic RLC re-enactment utilizing as it were CCCII and coasting capacitors. The CCCII were used for resistor, inductor and capacitor realization in this way making it perfect for IC creation. Four CCC, one drifting, and one grounded capacitor were utilized in the circuit. This approach employments inclination current to give orthogonal control over the normal recurrence and quality factor. Because the output nodes have a large impedance, cascading is effective. Figure 26 displays the schematic of the circuit. Equations (102-106) provide the filter transfer functions, Q, and ω0.

$$\frac{I_{BP}}{I_{in}} = \frac{s\frac{1}{C_2R_{x1}}}{s^2 + s\frac{1}{C_2R_{x1}} + \frac{1}{R_{x2}R_{x3}C_1C_2}} \tag{102}$$

$$\frac{I_{LP}}{I_{in}} = \frac{\frac{1}{R_{x2}R_{x3}C_1C_2}}{s^2 + s\frac{1}{C_2R_{x1}} + \frac{1}{R_{x2}R_{x3}C_1C_2}} \tag{103}$$

$$\frac{I_{HP}}{I_{in}} = \frac{S^2}{s^2 + s\frac{1}{C_2R_{x1}} + \frac{1}{R_{x2}R_{x3}C_1C_2}} \tag{104}$$

$$\omega_o = \sqrt{\frac{1}{R_{x2}R_{x3}C_1C_2}} \tag{105}$$

$$Q = R_{x1}\sqrt{\frac{C_2}{R_{x2}R_{x3}C_1}} \tag{106}$$

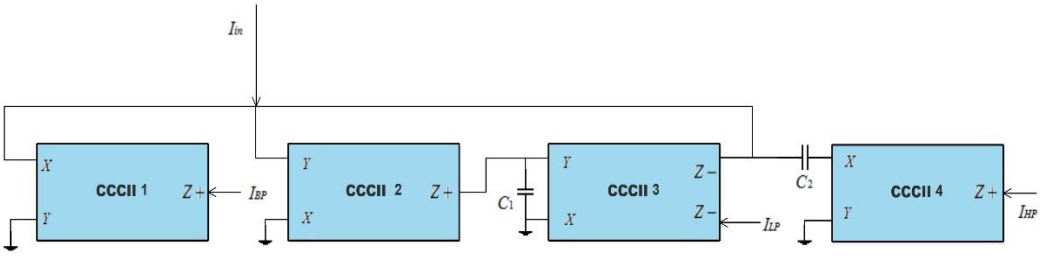

Figure 26: CCCII based filter topology [52].

A current mode biquadratic universal filter that can provide simultaneous HP, LP, and BP responses was well proposed by Siripruchyanun et al. [53]. Two capacitors and four CCCIIs are used in the filter.

Easy cascading results from the filter's output appearing at the high impedance nodes. Moreover, without changing its topology, the identical circuit can operate as an oscillator. The orthogonal control highlights of the quality calculation and characteristic recurrence through inclination current are extra advantages of this design. Furthermore, it is possible to separately alter the oscillator's frequency and oscillation condition. Additionally, no components that match the criterion apply. Figure 27 displays the schematic of the circuit. Equations (107-111) contain the filter transfer functions, Q, and ω_0.

$$\frac{I_{BP}}{I_{in}} = \frac{\frac{s}{C_1}\left(\frac{1}{R_{x2}} - \frac{1}{R_{x3}}\right)}{S^2 + \frac{s}{C_1}\left(\frac{1}{R_{x2}} - \frac{1}{R_{x3}}\right) + \frac{1}{R_{x4}R_{x3}C_1C_2}} \tag{107}$$

$$\frac{I_{LP}}{I_{in}} = \frac{\frac{1}{R_{x4}R_{x3}C_1C_2}}{S^2 + \frac{s}{C_1}\left(\frac{1}{R_{x2}} - \frac{1}{R_{x3}}\right) + \frac{1}{R_{x4}R_{x3}C_1C_2}} \tag{108}$$

$$\frac{I_{HP}}{I_{in}} = \frac{S^2}{S^2 + \frac{s}{C_1}\left(\frac{1}{R_{x2}} - \frac{1}{R_{x3}}\right) + \frac{1}{R_{x4}R_{x3}C_1C_2}} \tag{109}$$

$$\omega_o = \sqrt{\frac{1}{R_{x4}R_{x3}C_1C_2}} \tag{110}$$

$$Q = \frac{R_{x2}R_{x3}}{R_{x3} - R_{x2}}\sqrt{\frac{C_1}{R_{x4}R_{x3}C_2}} \tag{111}$$

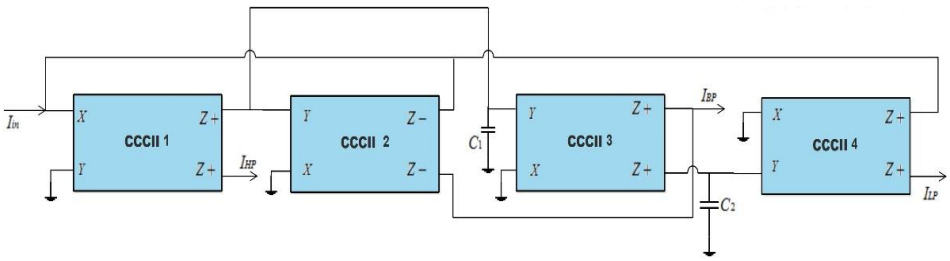

Figure 27: Filter topology [53]

DOCCCII was utilized by Abbas et al. [54] to develop a current-mode biquadratic widespread filter. Since, as it were, two capacitors were utilized, the usage was characterized by fewer inactive components. The filter delivered LP, HP, and BP reactions by utilizing the built-in parasitic resistance at the DOCCCII's X terminal. The HP, LP, and BP yield hubs can be tied together to provide the AP reaction, and the HP and LP hubs can be tied together to deliver the score reaction. Inclination current can be utilized to alter the filter's recurrence and quality figure. Figure 28 shows the circuit schematic, and the filter exchange capacities, Q, ω_0, and transfer speed are given by Conditions (112–119).

$$\frac{I_{BP}}{I_{in}} = \frac{s\frac{1}{C_1R_{x1}}}{s^2 + s\frac{1}{C_1R_{x1}} + \frac{1}{R_{x1}R_{x2}C_1C_2}} \tag{112}$$

$$\frac{I_{LP}}{I_{in}} = \frac{-\frac{1}{R_{x1}R_{x2}C_1C_2}}{s^2 + s\frac{1}{C_1R_{x1}} + \frac{1}{R_{x1}R_{x2}C_1C_2}} \tag{113}$$

$$\frac{I_{HP}}{I_{in}} = \frac{-S^2}{s^2 + s\frac{1}{C_1R_{x1}} + \frac{1}{R_{x1}R_{x2}C_1C_2}} \tag{114}$$

$$\frac{I_{BR}}{I_{in}} = \frac{-(S^2 + \frac{1}{R_{x1}R_{x2}C_1C_2})}{s^2 + s\frac{1}{C_1R_{x1}} + \frac{1}{R_{x1}R_{x2}C_1C_2}} \quad (115)$$

$$\frac{I_{AP}}{I_{in}} = \frac{-(S^2 - s\frac{1}{C_1R_{x1}} + \frac{1}{R_{x1}R_{x2}C_1C_2})}{s^2 + s\frac{1}{C_1R_{x1}} + \frac{1}{R_{x1}R_{x2}C_1C_2}} \quad (116)$$

$$\omega_o = \sqrt{\frac{1}{R_{x1}R_{x2}C_1C_2}} \quad (117)$$

$$Q = \sqrt{\frac{R_{x1}C_1}{R_{x2}C_2}} \quad (118)$$

$$\text{B.W.} = \frac{1}{R_{x1}C_1} \quad (119)$$

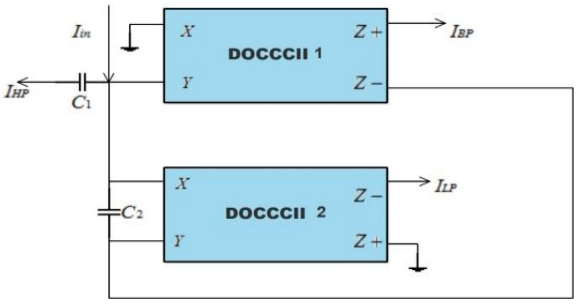

Figure 28: DOCCCII based filter topology [54].

Cao et al. [55] introduced cascaded current differencing units (CCDU), a novel active element for the application of higher-order filters. The CCCII was used to create the new active element. By adding grounded capacitors to the CCDU, the nth-order filter can be implemented using CCDU. The authors proposed a third-order filter with three grounded capacitors, as seen in Figure 29, which may simultaneously realize HP, LP, and BP reactions. This modern usage utilizing CCDU is able of diminishing the channel, realizing complexity incredibly. The filter exchange capacities are given in Conditions (120-124).

$$I_{LP} = \frac{1}{D(s)} I_{in} \quad (120)$$

$$I_{HP} = \frac{S^3C_1C_2C_3R_{x2}R_{x3}R_{x4}}{D(s)} I_{in} \quad (121)$$

$$I_{BP} = \frac{S^2C_1C_2R_{x2}R_{x3}}{D(s)} I_{in} \quad (122)$$

$$D(s) = S^3C_1C_2C_3R_{x2}R_{x3}R_{x4} + S^2C_1C_2R_{x2}R_{x3} + SC_2R_{x3+1} \quad (123)$$

$$\omega_o = \sqrt{\frac{1}{R_{x1}R_{x2}C_1C_2}} \quad (124)$$

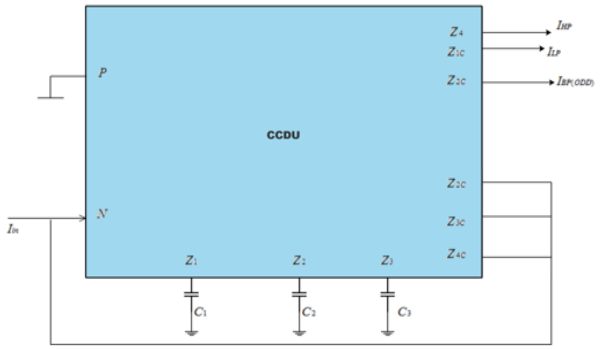

Figure 29: CCDU based filter topology [55].

Ozogus et al. [56] propose an execution of SIMO sort widespread filter that also uses threeICCII, two capacitors, and two resistors, all of which are drifting. To begin with, arranging all pass area serves as the establishment for the structure. The LP, BP, and HP reactions can all be realized at the same time by the filter. Include the LP and BP yield streams to obtain the score reaction. Moreover, by altering the BP current and including it in the LP and HP yield an AP reaction can, moreover, be created. The yields are all on the tall impedance hub, making it perfect for cascading. The major downside of the execution lies in the utilization of detached coasting components. The circuit schematic appears in Figure 30, and the conditions (125-130) allow the filter exchange capacities.

$$I_{0LP} = -\frac{1/R_1C_1R_2C_2}{D(s)} I_{in} \tag{125}$$

$$I_{0BP} = -\frac{s/C_2R_1}{D(s)} I_{in} \tag{126}$$

$$I_{0HP} = -\frac{S^2}{D(s)} I_{in} \tag{127}$$

$$D(s) = \frac{S^2C_1C_2R_1R_2 + sC_1R_2 + 1}{R_1C_1R_2C_2} \tag{128}$$

$$\omega_o = \sqrt{\frac{1}{R_1R_2C_1C_2}} \tag{129}$$

$$Q = \sqrt{\frac{C_2R_1}{R_2C_1}} \tag{130}$$

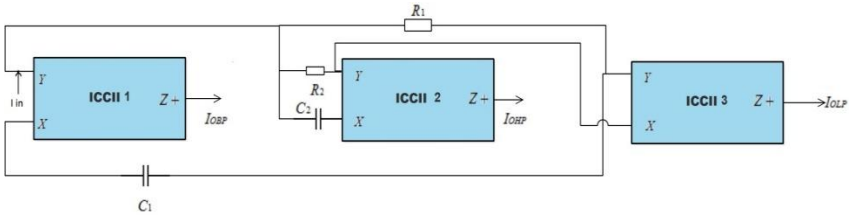

Figure 30: ICCII based filter topology [56].

Minaei et al. [57] describe a circuit for an electronically controllable current mode filter. Four NMOS transistors, two grounded capacitors, and three DXCCII were utilized in the circuit as straight resistors that worked in the triode locale with a resistance $R_i = \frac{1}{Kni(V_{ci}-V_{tn})}$

The resistance can be balanced by changing the control voltage Vci. The recommended filter was made by utilizing a KHN filter development, which comprises a summer/subtractor and two trustworthiness. LP, BP, and HP reactions are given by the filter. The appropriate yield streams can be

included to deliver the score and AP. The channel is fitting for cascading because of its moo input and high output impedances. Besides, it is conceivable to independently alter the filter's transfer speed, quality figure, and recurrence. Figure 31 shows the schematic of the circuit. Conditions (131–136) contain the filter exchange capacities, Q, and ω_0.

$$\frac{I_{BP}}{I_{in}} = \frac{-\frac{2(R_1+R_4)}{C_1R_1R_2}s}{s^2+\frac{2(R_1+R_4)}{C_1R_1R_2}s+\frac{4(R_1+R_4)}{C_1C_2R_1R_2R_3}} \tag{131}$$

$$\frac{I_{LP}}{I_{in}} = \frac{\frac{4(R_1+R_4)}{C_1C_2R_1R_2R_3}}{s^2+\frac{2(R_1+R_4)}{C_1R_1R_2}s+\frac{4(R_1+R_4)}{C_1C_2R_1R_2R_3}} \tag{132}$$

$$\frac{I_{HP}}{I_{in}} = \frac{s^2\frac{R_4}{R_1}}{s^2+\frac{2(R_1+R_4)}{C_1R_1R_2}s+\frac{4(R_1+R_4)}{C_1C_2R_1R_2R_3}} \tag{133}$$

$$\omega_o = 2\sqrt{\frac{(R_1+R_4)}{C_1C_2R_1R_2R_3}} \tag{134}$$

$$Q = \sqrt{\frac{C_1R_1R_2}{C_2R_3(R_1+R_4)}} \tag{135}$$

$$\text{B.W.} = \frac{2(R_1+R_4)}{C_1R_1R_2} \tag{136}$$

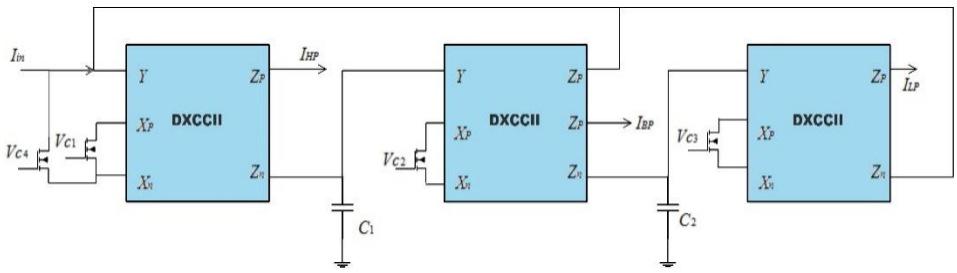

Figure 31: DXCCII based filter topology [57].

A current mode universal filter was presented by Alzaher et al. [4]. The utilization of unity gain cells serves as the foundation for the execution [58]. In Figure 32, the filter topology is displayed. By appropriately turning switches S_1 through S_3 ON and OFF, any filter function can be digitally selected at the output. Three floating resistors, two grounded capacitors, two non-programmable current followers (CF), two unity voltage followers (VF), and four digitally controllable current followers (DCCF) make up the filter structure. The implementation may independently control the frequency and quality factor digitally. Equations (137-141) provide the expression for Q and ω_o as well as the filter transfer functions. Keep in mind that mixed mode signal processing is the perfect application for this filter. The usage of floating resistors is the main problem, and control switch design must be done carefully to avoid introducing undesirable elements into the filter response.

$$\frac{I_{HP}}{I_{IN}} = -\alpha_4\frac{S^2}{S^2+s\,\alpha_1\alpha_3/C_1\,R_1+\alpha_1\alpha_2/C_1C_2R_2R_3} \tag{137}$$

$$\frac{I_{BP}}{I_{IN}} = \alpha_4 \frac{s\,\alpha_1\alpha_3/C_1 R_1}{S^2 + s\,\alpha_1\alpha_3/C_1 R_1 + \alpha_1\alpha_2/C_1C_2R_2R_3} \tag{138}$$

$$\frac{I_{LP}}{I_{IN}} = -\alpha_4 \frac{\alpha_1\alpha_2/C_1 R_2R_3C_2}{S^2 + s\,\alpha_1\alpha_3/C_1 R_1 + \alpha_1\alpha_2/C_1C_2R_2R_3} \tag{139}$$

$$\omega_o = \sqrt{\frac{\alpha_1\alpha_2}{C_1C_2R_2R_3}} \tag{140}$$

$$Q = \frac{R_1}{\alpha_3}\sqrt{\frac{C_1\alpha_2}{\alpha_1C_2R_2R_3}} \tag{141}$$

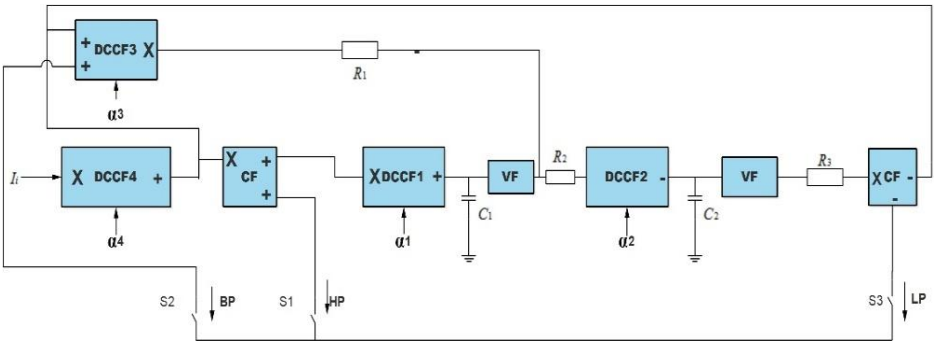

Figure 32: DCCF based filter topology [4].

Singh et al. provide an outstanding digitally programmable universal filter (DPUF) [59]. Current mode (CM), voltage mode (VM), trans-admittance mode (TAM), and trans-impedance mode (TIM) are the four modes in which the implementation can function. Digitally programmable current conveyors (DPCC) are used to create the circuit. The n-bit current division/summing network (CDN/CSN) is used by the DPCC to offer current amplification or attenuation. The magnitude of current attenuation (-) / amplification (+) is indicated by the control bits and the sign of parameter K. Six DPCC, two MOCCII, four grounded resistors, and two grounded capacitors make up the suggested DPUF. Four unique structures that function in all four modes as special cases can also be produced from this technique. The usage of all filter reactions in all four modes, separately programmable filter settings, utilization of all grounded detached components, need of components that fit necessities, and basic cascade are the topology's essential characteristics. Figure 33 (a-e) shows the generalized DPUF structure as well as four subsidiary structures. Conditions (142–145) constitute, as it were, the exchange work of the generalized DPUF. Conditions recommend that all the parameters, such as filter pickup, Q, and ωo, can be independently balanced utilizing advanced words. The filter's comprehensive programming grouping is given in Table 10. Organizing the examination can be utilized to get the exchange work, Q, and ωo for the remaining inferred structures.

$$V_O = I_O R_L \tag{142}$$

$$I_O = -\frac{S^2(K_1) - s\frac{1}{C_2R_2}\frac{K_6}{K_4}(K_2) + \frac{K_5K_6}{C_1C_2R_1R_2}(K_3)\left(I_i + \frac{V_i}{R_3}\right)}{S^2 + s\frac{1}{C_2R_2}\frac{K_6}{K_4} + \frac{K_5K_6}{C_1C_2R_1R_2}} \tag{143}$$

For implementation of the filter $K_5 = K_6$ is set in the above equation. Where, parameter K is the decimal equivalent of the applied digital code word.

$$\omega_o = K_5\sqrt{\frac{1}{C_1C_2R_2R_1}} \tag{144}$$

$$Q = K_4\sqrt{\frac{C_2R_2}{C_1R_1}} \qquad (145)$$

Table 10: Filter input excitation sequence

Filter Function	Digital Codeword	Gain parameters in different modes			
		TAM	CM	TIM	VM
HP	K_5=K_3=0, K_1≠0	K_1/R_3	K_1	K_1R_L	K_1R_L/R_3
BP	K_1=K_3=0, K_2≠0	K_2/R_3	K_2	K_2R_L	K_2R_L/R_3
LP	K_1=K_2=0, K_3≠0	K_3/R_3	K_3	K_3R_L	K_3R_L/R_3
BR	K_1=K_3≠0, K_2=0	K_1/R_3	K_1	K_1R_L	$K_1/R_3 R_L$
AP	K_1=K_2=K_3≠0	K_1/R_3	K_1	K_1R_L	K_1R_L/R_3

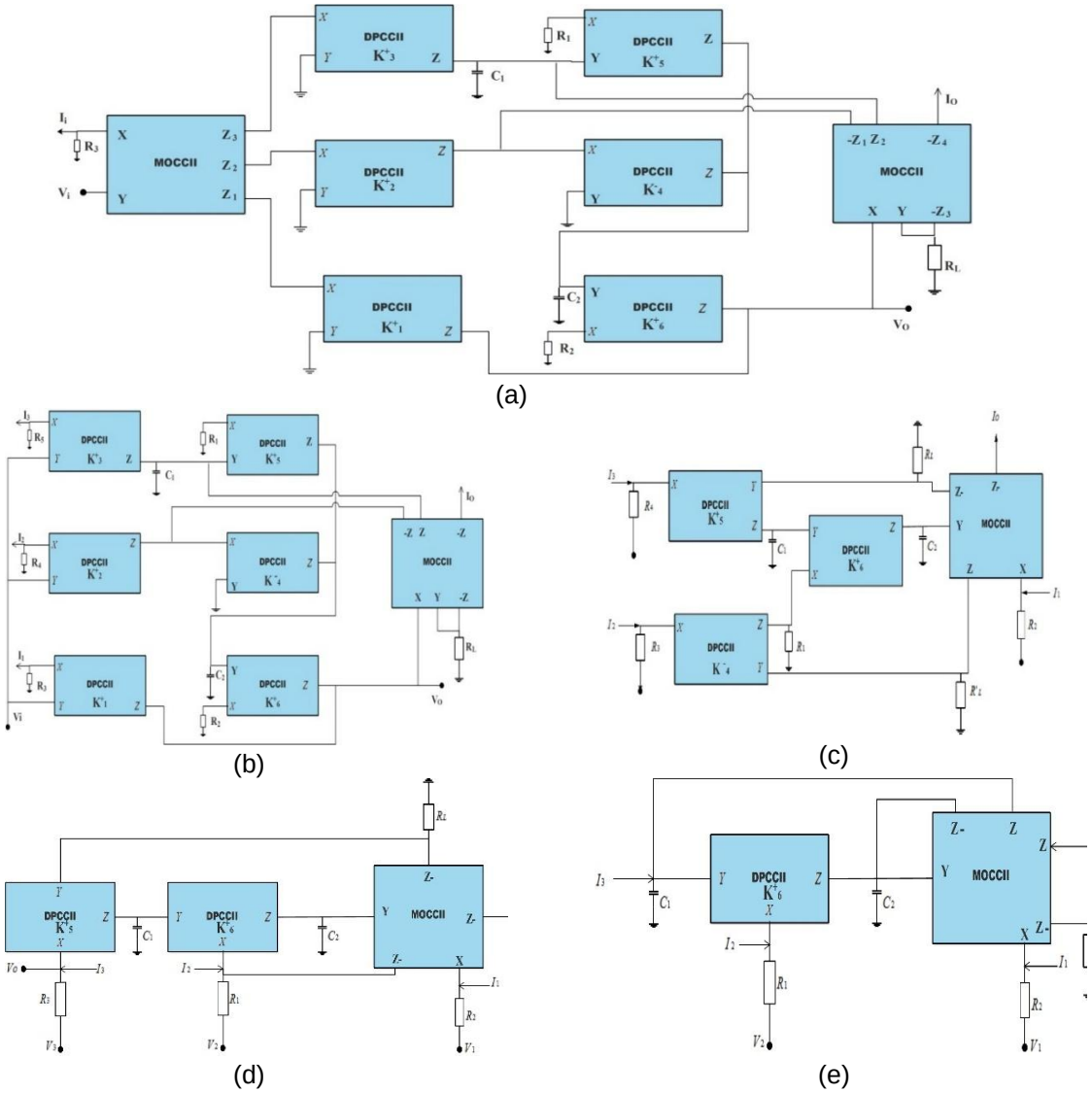

Figure 33: DPCC based filter topologies proposed in [59] (a) Generalized DPUF structure (b) To begin with inferred structure (c) Moment inferred structure (d) Third inferred structure (e) Fourth determined structure.

Ask et al. [60] presented a biquadratic filter based on DPCCII that can at the same time realize HP, LP, and BP reactions. Three DPCCII, two grounded capacitors, and four grounded resistors were utilized in the filter. The advanced control word permits isolated alteration of the post-recurrence and

quality figure. It is suitable for IC execution due to the grounded components. In Figure 34, the circuit appears. The circuit examination yields current exchange capacities (146–150).

$$\frac{\mathrm{I}_{HP}}{\mathrm{I}_{IN}} = \frac{S^2}{S^2 + s\,N_1R_3/N_2C_2R_4\,R_1 + N_1N_2/C_1C_2R_2R_1} \tag{146}$$

$$\frac{\mathrm{I}_{LP}}{\mathrm{I}_{IN}} = \frac{N_1N_2/C_1C_2R_2R_1}{S^2 + s\,N_1R_3/N_2C_2R_4\,R_1 + N_1N_2/C_1C_2R_2R_1} \tag{147}$$

$$\frac{\mathrm{I}_{BP}}{\mathrm{I}_{IN}} = \frac{s(N_1R_3)/N_3C_2R_4\,R_1}{S^2 + s\,N_1R_3/N_2C_2R_4\,R_1 + N_1N_2/C_1C_2R_2R_1} \tag{148}$$

$$\omega_o = \sqrt{N_1N_2/C_1C_2R_2R_1} \tag{149}$$

$$Q = \frac{N_3R_4}{R_3}\sqrt{\frac{N_2C_2R_1}{N_1C_1R_2}} \tag{150}$$

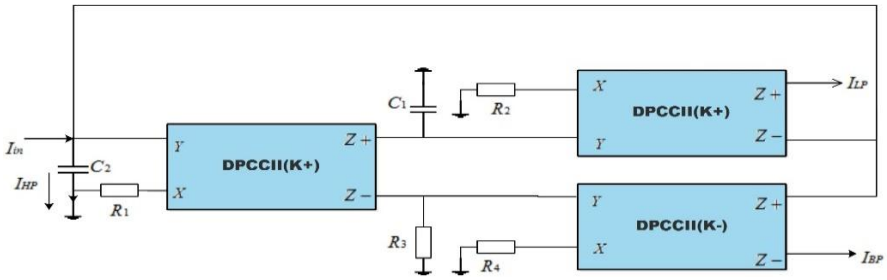

Figure34: DPCCII based filter topology [60].

Two classes of universal filters are studied. The MIMO type filters cannot realize all the filter responses simultaneously while SIMO filters can realize all the function at the same time and hence are suitable for reconfigurable systems. Table 11 provides a thorough comparison of the various filter architectures discussed previously.

Table 11: Comparison of various filter structures.

Ref.	Type of Filter	No. of grounded/floating passive elements		Programmability/Type (Analog or Digital)	No. and type of active elements	High Impedance output node
		Grounded C/R	Floating C/R			
[4]	SIMO	2/0	0/3	Digital	4-DCCF, 2-CF&2-VF	Yes
[36]	MISO	2/0	-	Analog (bias current)	2-CCCCTA	Yes
[37]	MISO	2/0	-	Analog (bias current)	2 -CCTA	Yes
[38]	MIMO	2/3	-	No	3-MOICCII	Yes
[39]	MISO	2/0	-	Analog (bias current)	2-MOCCCII	Yes
[40]	MISO	2/0	-	Analog (bias current)	3-DOCCCII	Yes
[41]	MISO	2/2	0/1	No	3-MOCCII	Yes
[41]	MISO	2/1	0/1	No	3-MOCCII	Yes
[41]	MISO	2/3	-	No	3-MOCCII	Yes
[42]	MISO	2/1	0/1	No	3-ICCII	Yes
[43]	MISO	2/0	-	Analog (bias current)	3-MOCCCII	Yes
[44]	SIMO	2/1	0/1	No	2-CCII+	No
[45]	SIMO	2/1	0/1	No	2-CCII-	No
[46]	SIMO	2/4	-	No	3-MOCCII	Yes

[47]	SIMO	2/0	0/2	Analog (bias current)	3-ECCII	Yes
[48]	SIMO	3/0	-	Analog (bias current)	5- CCCII	Yes
[49]	SIMO	2/0	-	Analog (bias current)	2-CCII & 2 OTA	Yes
[50]	SIMO	-	2/2	No	4-CCII	Yes
[51]	SIMO	2/8	-	No	7-CCII	Yes
[52]	SIMO	1/0	1/0	Yes	4-CCCII	Yes
[53]	SIMO	2/0	-	Yes	4-CCCII	Yes
[54]	SIMO	-	2/0	Yes	2-DOCCCII	Yes
[55]	SIMO	3/0	-	Yes	1-CCDU	Yes
[56]	SIMO	-	2/2	No	3-ICCII	Yes
[57]	SIMO	2/0	-	Analog (voltage controlled resistors)	3-DXCCII	Yes
[59]	SIMO	2/4	-	Digitally Programmable	6-DPCC,2-MOCCII	Yes
[60]	SIMO	2/4	-	Digitally Programmable	3-DPCC	Yes

Conclusions

This article examines the design restrictions for universal filters. Some common current mode active elements with CCII as their fundamental building block are briefly introduced. On the premise of these dynamic components, twenty-five extraordinary current. mode widespread filters are inspected and assessed. The least number of dynamic and inactive components utilized, the number of grounded and coasting detached components, the autonomous tunability of the filter's recurrence and quality calculate, and programmability are the criteria utilized to compare the filter structures. The think about emphasized the distinctive approaches the analysts utilized to synthesize the filters. The ponder proposes that the three most vital plan contemplations when planning a filter are the least sum of dynamic and inactive components and free control of the filter parameters. Moreover, it may be said that including computerized programmability to filters will permit for blended mode flag preparing on a single chip and donate the filter structure adaptability.

References

[1] M. Almamoori, M. Almaktar, M. Khaleel, F. Mohamed, and A. Elbreki, “Assessing STATCOM-enabled reactive power control in fragile power transmission systems: A case study perspective,” Math. Model. Eng. Probl., vol. 11, no. 8, pp. 2019–2028, 2024.

[2] M. Khaleel et al., “The impact of SMES integration on the power grid: Current topologies and nonlinear control strategies,” in New Technologies, Development and Application VII, Cham: Springer Nature Switzerland, 2024, pp. 108–121.

[3] R. Senani, D. Bhaskar, and A. Singh, Current Conveyors: Variants, Applications and Hardware Implementations. Springer, 2014.

[4] H. A. Alzaher, “A CMOS digitally programmable universal current-mode filter,” IEEE Trans. Circuits Syst. II: Express Briefs, vol. 8, pp. 758–762, 2008.

[5] P. A. Mohan, Current-Mode VLSI Analog Filters: Design and Applications. Springer Science & Business Media, 2012.

[6] M. Faseehuddin, J. Sampe, and S. Islam, “Schmitt trigger based on dual output current controlled current conveyor in 16nm CMOS technology for digital applications,” in Proc. IEEE Int. Conf. Semiconductor Electronics (ICSE), 2016, pp. 82–85.

[7] M. Kumngern, F. Khateb, T. Kulej, M. Kyselak, S. Lerkvaranyu, and B. Knobnob, “Current-mode shadow filter with single-input multiple-output using current-controlled current conveyors with controlled current gain,” Sensors, vol. 24, no. 2, p. 460, 2024.

[8] M. Faseehuddi, J. Sampe, and M. S. Islam, “Designing ultra low voltage low power active analog blocks for filter applications utilizing the body terminal of MOSFET: A review,” Asian J. Sci. Res., vol. 9, pp. 106–121, 2016.

[9] F. Majeed and M. Yasin, “A novel voltage comparator and its application—A new simple configuration based on 45 nm 2nd generation CMOS current controlled current conveyor,” Acta Electrotehnica, vol. 53, 2012.

[10] C. Shekhar, N. Pandey, and P. Jain, “Compact realization of MISO shadow filters based on DDCC,” AEU–Int. J. Electron. Commun., 2025, Art. no. 155933.

[11] K. D. Sharma, K. Pal, and C. Psychalinos, “A resistorless high input impedance first order all-pass filter using CCCIIs,” World Acad. Sci. Eng. Technol., Int. J. Electr. Comput. Energetic Electron. Commun. Eng., vol. 7, pp. 213–215, 2013.
[12] H. Schmid and G. S. Moschytz, “Tunable CCII MOSFET filter biquads for video frequencies,” in Proc. Eur. Conf. Circuit Theory Design, 1997, pp. 82–87.
[13] M. Khaleel et al., “An optimization approaches and control strategies of hydrogen fuel cell systems in EDG-integration based on DVR technology,” J. Eur. Syst. Autom., vol. 57, no. 2, pp. 551–565, 2024.
[14] S. Minaei, “A new high performance CMOS third generation current conveyor (CCIII) and its application,” Electr. Eng., vol. 85, pp. 147–153, 2003.
[15] A. Fabre, O. Saaid, F. Wiest, and C. Boucheron, “Current controlled bandpass filter based on translinear conveyors,” Electron. Lett., vol. 31, pp. 1727–1728, 1995.
[16] M. Siripruchyanun and W. Jaikla, “Current controlled current conveyor transconductance amplifier (CCCCTA): A building block for analog signal processing,” Electr. Eng., vol. 90, pp. 443–453, 2008.
[17] A. A. El-Adawy, A. M. Soliman, and H. O. Elwan, “A novel fully differential current conveyor and applications for analog VLSI,” IEEE Trans. Circuits Syst. II: Analog Digit. Signal Process., vol. 47, pp. 306–313, 2000.
[18] F. Kacar, B. Metin, and H. Kuntman, “A new CMOS dual-x second generation current conveyor (DXCCII) with an FDNR circuit application,” AEU–Int. J. Electron. Commun., vol. 64, pp. 774–778, 2010.
[19] H. Elwan and A. Soliman, “Novel CMOS differential voltage current conveyor and its applications,” IEE Proc. Circuits Devices Syst., vol. 144, pp. 195–200, 1997.
[20] M. Altun, H. Kuntman, S. Minaei, and O. K. Sayin, “Realisation of n th-order current transfer function employing ECCIIs and application examples,” Int. J. Electron., vol. 96, pp. 1115–1126, 2009.
[21] I. A. Khan, M. Khan, and N. Afzal, “Digitally programmable multifunctional current mode filter using CCIIs,” J. Active Passive Electron. Devices, vol. 1, pp. 213–220, 2006.
[22] G. Ferri and N. C. Guerrini, Low-Voltage Low-Power CMOS Current Conveyors. Springer, 2003.
[23] M. Khaleel, N. El-Naily, H. Alzargi, M. Amer, T. Ghandoori, and A. Abulifa, “Recent progress in synchronization approaches to mitigation voltage sag using HESS D-FACTS,” in Proc. Int. Conf. Emerging Trends Eng. Med. Sci. (ICETEMS), 2022.
[24] M. M. Khaleel, M. R. Adzman, and S. M. Zali, “An integrated of hydrogen fuel cell to distribution network system: Challenging and opportunity for D-STATCOM,” Energies, vol. 14, no. 21, p. 7073, 2021.
[25] M. M. Khaleel, M. R. Adzman, S. M. Zali, M. M. Graisa, and A. A. Ahmed, “A review of fuel cell to distribution network interface using D-FACTS: Technical challenges and interconnection trends,” Int. J. Electr. Electron. Eng. Telecommun., pp. 319–332, 2021.
[26] H. Alzaher, N. Tasadduq, and O. Al-Ees, “Implementation of reconfigurable nth-order filter based on CCII,” Analog Integr. Circuits Signal Process., vol. 75, pp. 539–545, 2013.
[27] S. A. Mahmoud, M. A. Hashiesh, and A. M. Soliman, “Low-voltage digitally controlled fully differential current conveyor,” IEEE Trans. Circuits Syst. I: Reg. Papers, vol. 52, pp. 2055–2064, 2005.
[28] S. M. Al-Shahrani and M. A. Al-Gahtani, “A new polyphase current-mode filter using digitally-programmable CCCII,” in Proc. Int. Conf. Microelectronics, 2006, pp. 142–145.
[29] Z. Abbas, M. Yakupov, N. Olivieri, A. Ripp, and G. Strobe, “Yield optimization for low power current controlled current conveyor,” in Proc. Symp. Integr. Circuits Syst. Design (SBCCI), 2012, pp. 1–6.
[30] J. Dunning-Davies and F. Stephenson, “Sensitivity optimization of active filters containing current conveyors and controlled sources,” Int. J. Electron., vol. 48, pp. 283–289, 1980.
[31] M. A. Albrni, J. Sampe, S. H. M. Ali, and A. R. M. Zain, “Design of VD-DDCC for novel dual mode universal filter with grounded passive components,” Int. J. Nanoelectron. Mater., vol. 13, pp. 259–266, 2020.
[32] A. Nieuwoudt, J. Kawa, and Y. Massoud, “Robust reconfigurable filter design using analytic variability quantification techniques,” in Proc. IEEE/ACM Int. Conf. Comput.-Aided Design, 2008, pp. 765–770.
[33] H. E. Graeb, Analog Design Centering and Sizing. Springer, 2007.
[34] M. Faseehuddin, M. A. Albrni, J. Sampe, and S. H. Ali, “Novel VDBA based universal filter topologies with minimum passive components,” J. Eng. Res., vol. 9, no. 3B, 2021.
[35] D. Singh, N. Afzal, D. Prasad, R. Srivastava, and K. Panwar, “Digitally programmable voltage mode universal filters-a minimal realization,” Circuits Syst., vol. 6, pp. 213, 2015.
[36] P. Suwanjan, S. Siripongdee, and W. Jaikla, “MISO current-mode biquad filter with independent control of pole frequency and quality factor,” Radioengineering, 2012.
[37] T. Thosdeekoraphat, S. Summart, C. Saetiaw, S. Santalunai, C. Thongsopa, and W. Jaikla, “Resistor-less current-mode universal biquad filter using CCTAs and grounded capacitors,” World Acad. Sci. Eng. Technol., vol. 69, pp. 559–563, 2012.

[38] H.-P. Chen, W.-Y. Huang, M.-Y. Hsieh, and K.-H. Wu, “Universal current mode biquadratic filter with two inputs and four outputs using ICCIIs,” in Proc. Int. Conf. Inf. Sci. Electron. Electr. Eng. (ISEEE), 2014, pp. 233–236.
[39] O. Channumsin, T. Pukkalanun, and W. Tangsrirat, “Universal current-mode biquad with minimum components,” in Proc. Int. Multi-Conf. Eng. Comput. Scientists, 2011.
[40] W. Tangsrirat and W. Surakampontorn, “High output impedance current-mode universal filter employing dual-output current-controlled conveyors and grounded capacitors,” AEU–Int. J. Electron. Commun., vol. 61, pp. 127–131, 2007.
[41] J.-W. Horng, “High output impedance current-mode universal biquadratic filters with five inputs using multi-output CCIIs,” Microelectron. J., vol. 42, pp. 693–700, 2011.
[42] M. Faseehuddin, N. Herencsar, M. A. Albrni, S. Shireen, and J. Sampe, “Electronically tunable mixed mode universal filter employing grounded capacitors utilizing highly versatile VD-DVCC,” Circuit World, vol. 48, no. 4, pp. 511–528, 2022.
[43] H.-P. Chen and P.-L. Chu, “Versatile universal electronically tunable current-mode filter using CCCIIs,” IEICE Electron. Express, vol. 6, pp. 122–128, 2009.
[44] A. Fabre and M. Alami, “Universal current mode biquad implemented from two second generation current conveyors,” IEEE Trans. Circuits Syst. I: Fundam. Theory Appl., vol. 42, pp. 383–385, 1995.
[45] D. Bhaskar, V. Sharma, M. Monis, and S. Rizvi, “New current-mode universal biquad filter,” Microelectron. J., vol. 30, pp. 837–839, 1999.
[46] M. Faseehuddin, M. A. Albrni, N. Herencsar, J. Sampe, and S. H. M. Ali, “Novel electronically tunable biquadratic mixed-mode universal filter capable of operating in MISO and SIMO configurations,” Informacije MIDEM, vol. 50, no. 3, pp. 189–204, 2020.
[47] S. Minaei, O. K. Sayin, and H. Kuntman, “A new CMOS electronically tunable current conveyor and its application to current-mode filters,” IEEE Trans. Circuits Syst. I: Reg. Papers, vol. 53, pp. 1448–1457, 2006.
[48] S. Minaei and S. Türköz, “Current-mode electronically tunable universal filter using only plus-type current controlled conveyors and grounded capacitors,” ETRI J., vol. 26, pp. 292–296, 2004.
[49] D. Biolek, M. Siripruchyanun, and W. Jaikla, “CCII and OTA based current–mode universal biquadratic filter,” in Proc. 6th PSU Eng. Conf., 2008, pp. 238–241.
[50] S. Ozoguz and C. Acar, “Universal current-mode filter with reduced number of active and passive components,” Electron. Lett., vol. 33, pp. 948–949, 1997.
[51] C.-M. Chang, “Universal active current filter with single input and three outputs using CCIIs,” Electron. Lett., vol. 29, pp. 1932–1933, 1993.
[52] S. Siripongdee, S. Tuntrakool, and W. Jaikla, “High output impedance current-mode universal filter with independent control of pole frequency and quality factor,” in Proc. 11th WSEAS Int. Conf. Instrum. Meas. Circuits Syst., 2012, pp. 88–92.
[53] N. T. C. T. M. Siripruchyanun, “CCCII-based high input-impedance current-mode universal filter and quadrature oscillator,” 2009.
[54] Z. Abbas, G. Scotti, and M. Olivieri, “Current controlled current conveyor (CCCII) and application using 65nm CMOS technology,” World Acad. Sci. Eng. Technol., vol. 55, pp. 935–939, 2011.
[55] M. Cao, H. He, H. Lin, H. Peng, and B. Zhu, “Current-mode n th-order filter based on a minimal component,” J. Circuits Syst. Comput., vol. 25, p. 1650035, 2016.
[56] S. Özoguz, A. Toker, and O. Çiçekogl, “First-order allpass sections-based current-mode universal filter using ICCIIs,” Electron. Lett., vol. 36, 2000.
[57] S. Minaei, “Electronically tunable current-mode universal biquad filter using dual-x current conveyors,” J. Circuits Syst. Comput., vol. 18, pp. 665–680, 2009.
[58] H. Alzaher and M. Ismail, “Current-mode universal filter using unity gain cells,” Electron. Lett., vol. 35, pp. 2198–2200, 1999.
[59] M. Faseehuddin, N. Herencsar, M. A. Albrni, and J. Sampe, “Electronically tunable mixed-mode universal filter employing a single active block and a minimum number of passive components,” Appl. Sci., vol. 11, no. 1, p. 55, 2020.
[60] P. Beg, I. A. Khan, M. Ansari, and A. M. Nahhas, “Low voltage digitally programmable current mode multifunctional filter,” Am. J. Signal Process., vol. 3, pp. 49–53, 2013.